

# Synthesis of Pyridyl Functionalized 3-Pyrolyl BODIPY based Fluoroprobes and Application Towards Highly Selective Detection of Picric Acid

Debendra Tewary<sup>1,2</sup>, Kanhu Charan Behera<sup>1</sup>, David R. Turner<sup>3\*</sup> and Mangalampalli Ravikanth<sup>1\*</sup>

<sup>1</sup>Department of Chemistry, IIT Bombay, Powai-400076, Mumbai, India

<sup>2</sup>IITB- Monash Research Academy, IIT Bombay, Powai-400076, Mumbai, India

<sup>3</sup>School of Chemistry, Monash University, Clayton, VIC 3800, Australia

## Contents

Sl. no	Details	Page no.
1.	Experimental: Materials and methods	S2-S3
2.	Characterization data of all synthesized compounds: Mass analysis, <sup>1</sup> H, <sup>13</sup> C, <sup>11</sup> B, <sup>19</sup> F NMR, COSY, NOESY	S4-S17
3.	Photophysical investigations:  UV and Fluorescence spectra compounds alone and in the presence of different nitroaromatics  Excited state lifetime data of all compounds  Comparison of sensing parameters of compound <b>5</b> with other reported molecules	S18-S24
4.	Theoretical calculations:  DFT optimized structure and data of <b>5</b> and <b>5+PA</b>  and TD-DFT data of <b>5</b> and <b>5+PA</b>	S25-S31
5.	References	S32

## **Materials and Methods**

### **Materials:**

The chemicals such as pyrrole, Pd(PPh<sub>3</sub>)<sub>4</sub>, BF<sub>3</sub>·Et<sub>2</sub>O, 3/4-pyridineboronic acids, methyl iodide, Na<sub>2</sub>CO<sub>3</sub>, 3-dichloro-5,6-dicyano-1,4-benzoquinone (DDQ), TFA, TEA, THF, toluene and acetonitrile were used as obtained from Sigma Aldrich and TCI. All other chemicals used for the synthesis were reagent grade unless otherwise specified. Column chromatography was performed on silica gel (mesh size-100-200) grade.

### **Methods:**

- The <sup>1</sup>H and <sup>13</sup>C NMR spectra were recorded in CDCl<sub>3</sub> on Bruker 400 and 500 MHz instruments. The frequencies for the <sup>13</sup>C nucleus are 100.06 and 125.77 MHz for 400 and 500 MHz instruments, respectively. Similarly, the frequencies for the <sup>11</sup>B and <sup>19</sup>F nucleus are 193 and 376 MHz for 400 MHz instruments.
- Absorption and steady state fluorescence spectra were obtained with PerkinElmer Lambda-35.
- Cyclic voltammetry (CV) studies were carried out with the BAS electrochemical system utilizing the three-electrode configuration consisting of glassy carbon (working electrode), platinum wire (auxiliary electrode), and saturated calomel (reference electrode) electrodes. The experiments were done in dry dichloromethane using tetrabutylammonium perchlorate as a supporting electrolyte.
- Mass spectra were recorded with an Agilent Q-TOF ESI mass spectrometer.

- Fluorescence quantum yields were determined<sup>S1</sup> in each case by comparing the corrected spectrum with that of Rhodamine 6G ( $\Phi = 0.95$ )<sup>S2</sup> in EtOH by taking the area under total emission using the procedure reported earlier.
- The exponential decay curve of **5** and **5+HPA** were fitted appropriately with a mono/biexponential equation  $Y = A + B_1 \exp(-t/\tau_1) + B_2 \exp(-t/\tau_2)$  to obtain best goodness-of-fit  $\chi^2$  value. The average life time ( $\tau_{av}$ ) was calculated following the equations depicted in literature<sup>S3</sup>.
- Quantum chemical calculations (gas phase/vacuum) for ground state energy minimized structures for the probes **5** and **5+PA** were done employing density functional theory (DFT) in a Gaussian 09W program package. The ground state structural elucidation involved in optimization using DFT-based Beck-3 Lee Young Parr (B3LYP) functional where 6-31+G (d,p) basis sets were used. To obtain the oscillator strengths, identical basis and functional hybrid set were used whereas the vertical excitation energies were obtained with the help of TD-DFT techniques. Under the Polarisable Continuum Model (PCM) in the CH<sub>2</sub>Cl<sub>2</sub> media, TD-DFT analysis were done using the Self-Consistent Reaction Field (SCRF). The electronic absorption spectra as well as the oscillator strengths were thoroughly examined using TD-DFT with PCM model based on the optimized structures in the S<sub>0</sub> state.

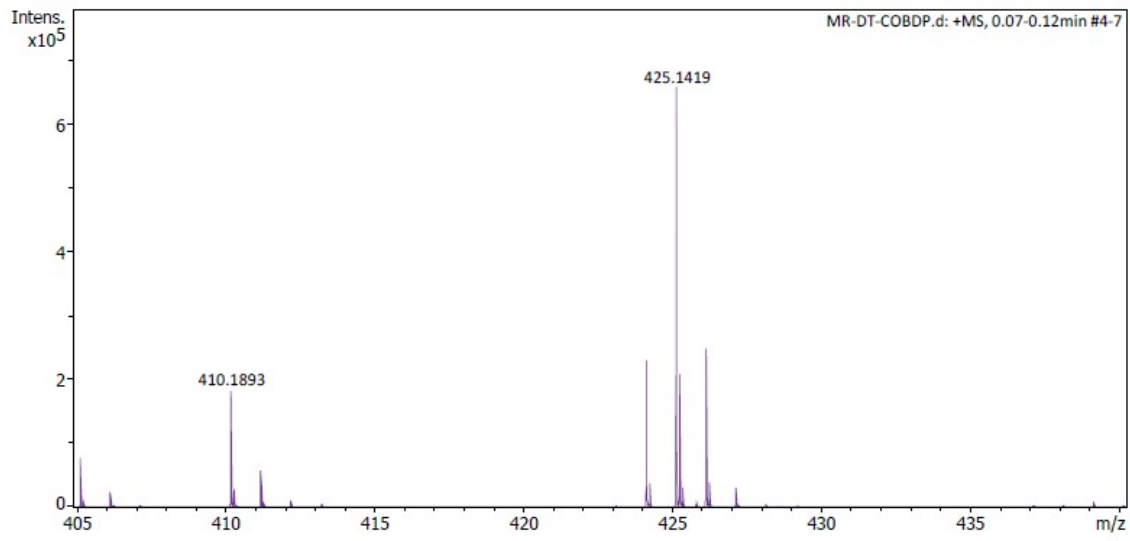


**Fig S1.** LRMS Spectrum of compound 3.

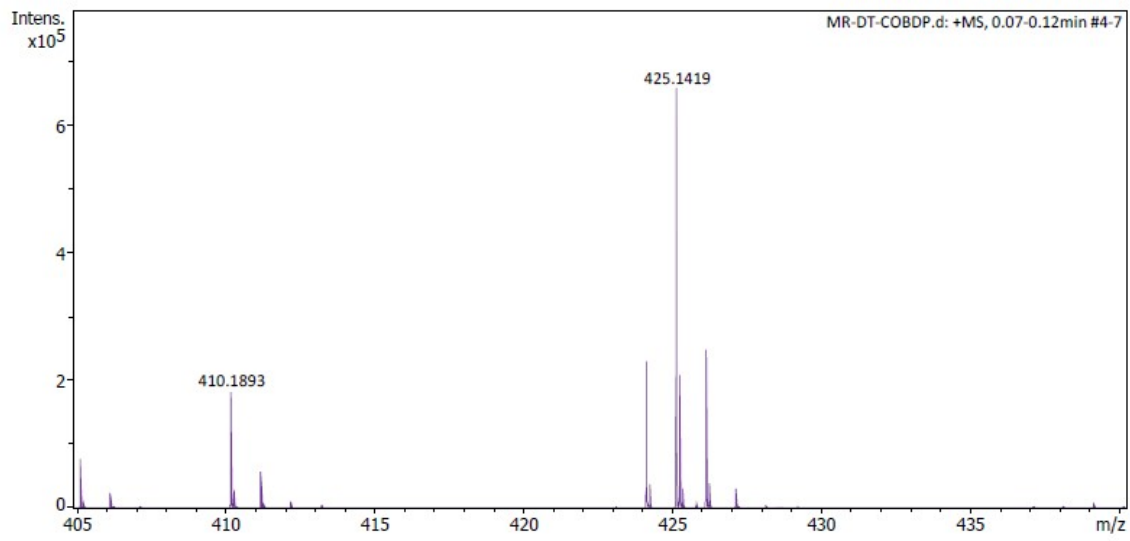


**Fig S2.** LRMS Spectrum of compound 4.

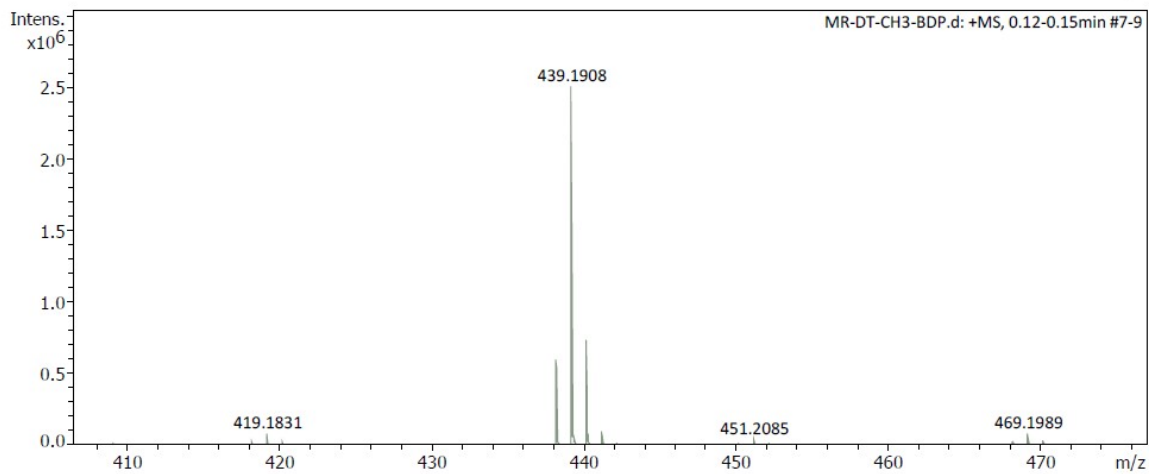


**Fig S3.** LRMS Spectrum of compound 5.



**Fig S4.** HRMS Spectrum of compound 6.

**Compound Details**

Cpd. 1: C24 H17 B F2 N4

Formula	m/z	Observed M/Z	Difference Da	Difference PPM	Score
C24 H17 B F2 N4	411.1595	411.159544122462	0.326769586251885	0.79864485166391	99.45

*Compound Spectra (Zoomed)*

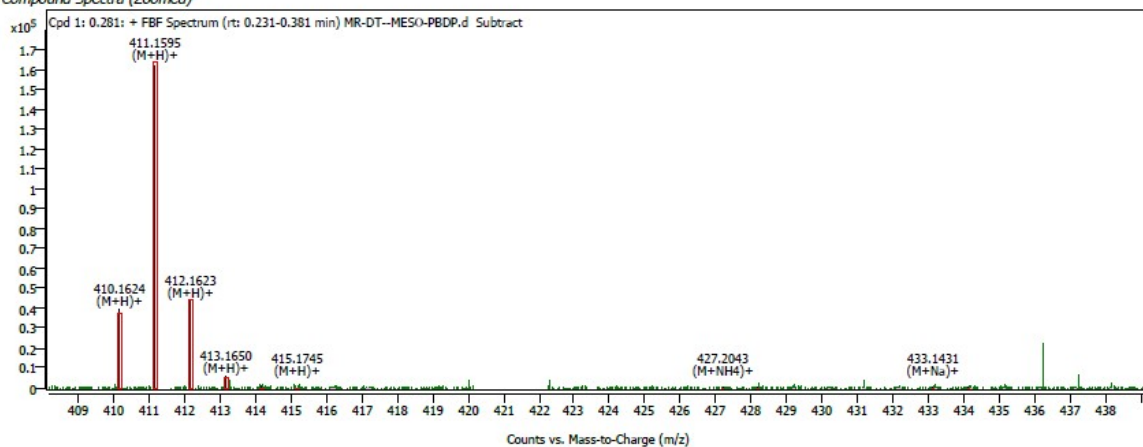


**Fig S5.** HRMS Spectrum of compound 7.



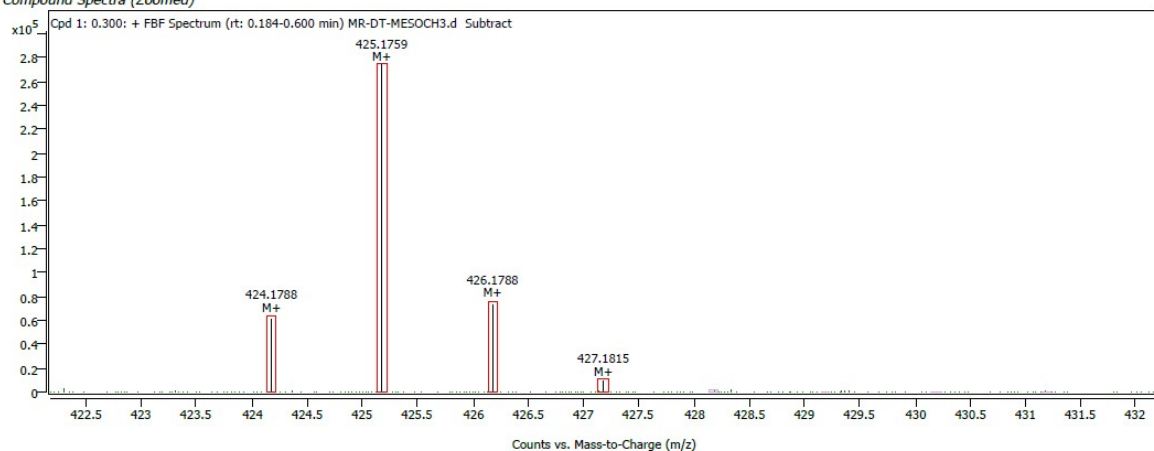
**Fig S6.** HRMS Spectrum of compound **8**.

**Compound Details**

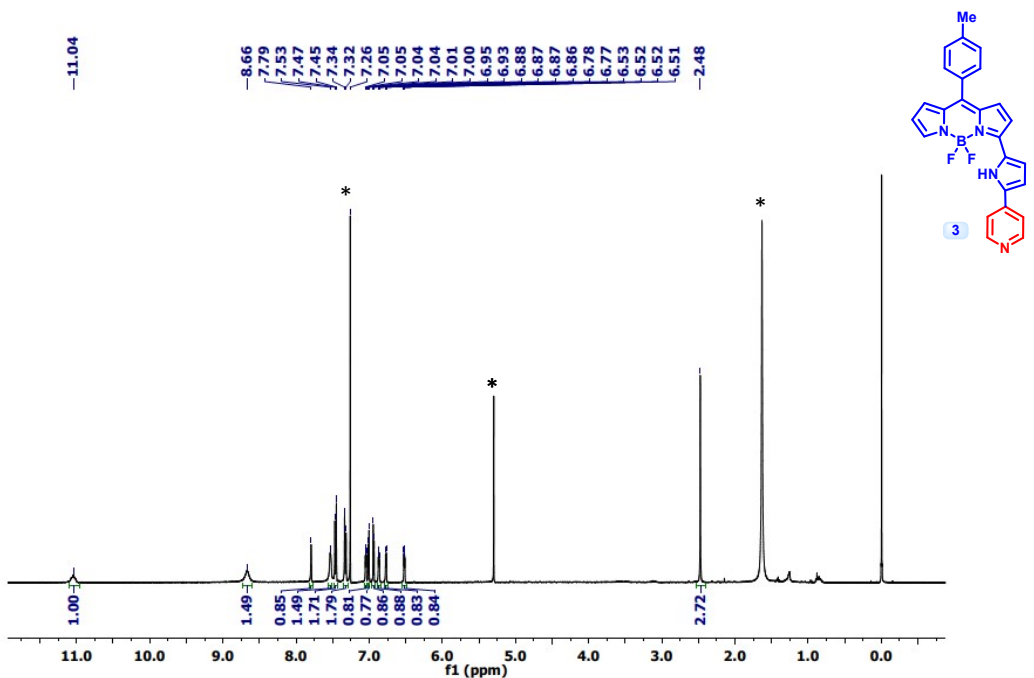
Cpd. 1: C25 H20 B F2 N4

Formula	m/z	Observed M/Z	Difference Da	Difference PPM	Score
C25 H20 B F2 N4	425.1759	425.175859276729	1.03970343030824	2.4510986102631	97.03

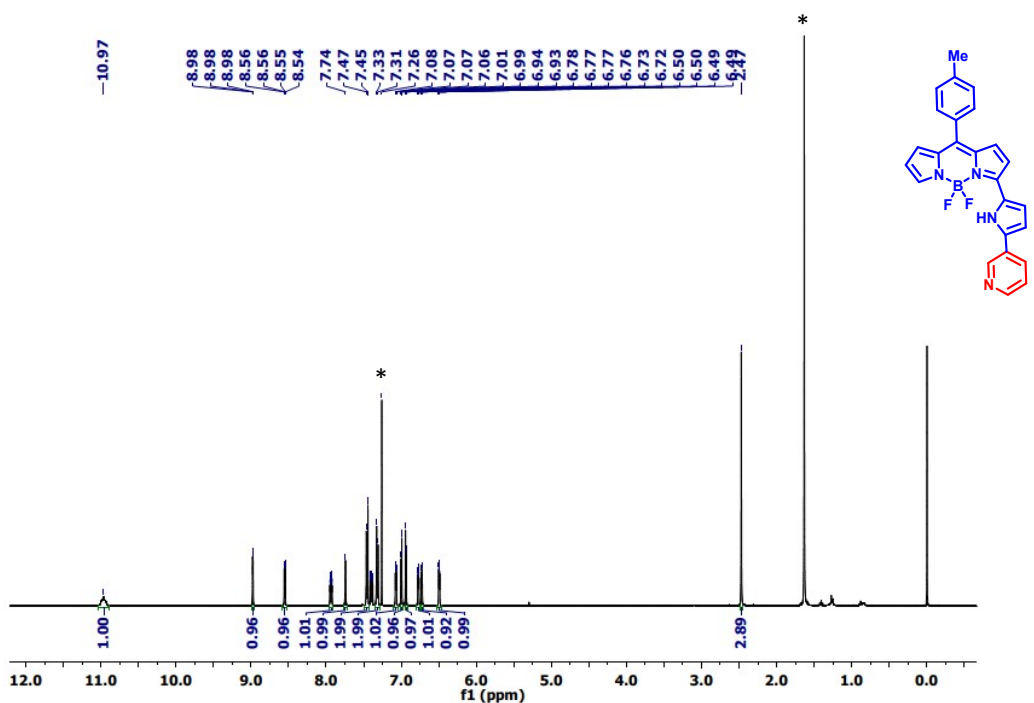
*Compound Spectra (Zoomed)*



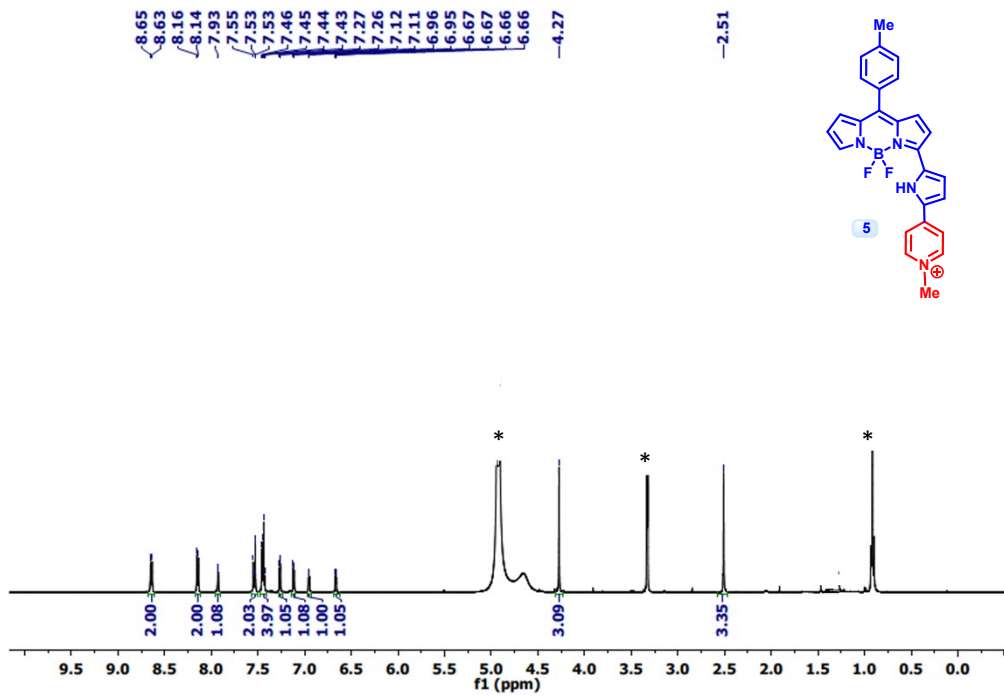
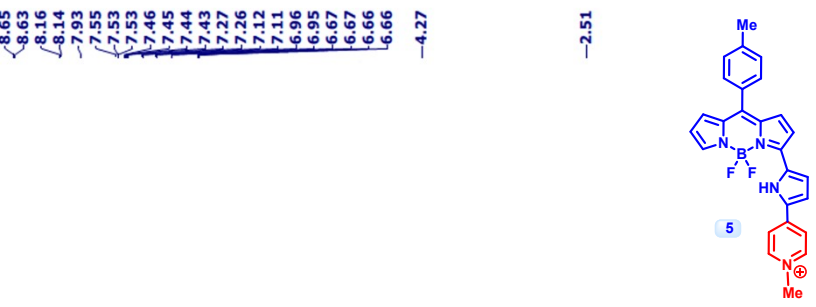
**Fig S7.** HRMS Spectrum of compound **9**



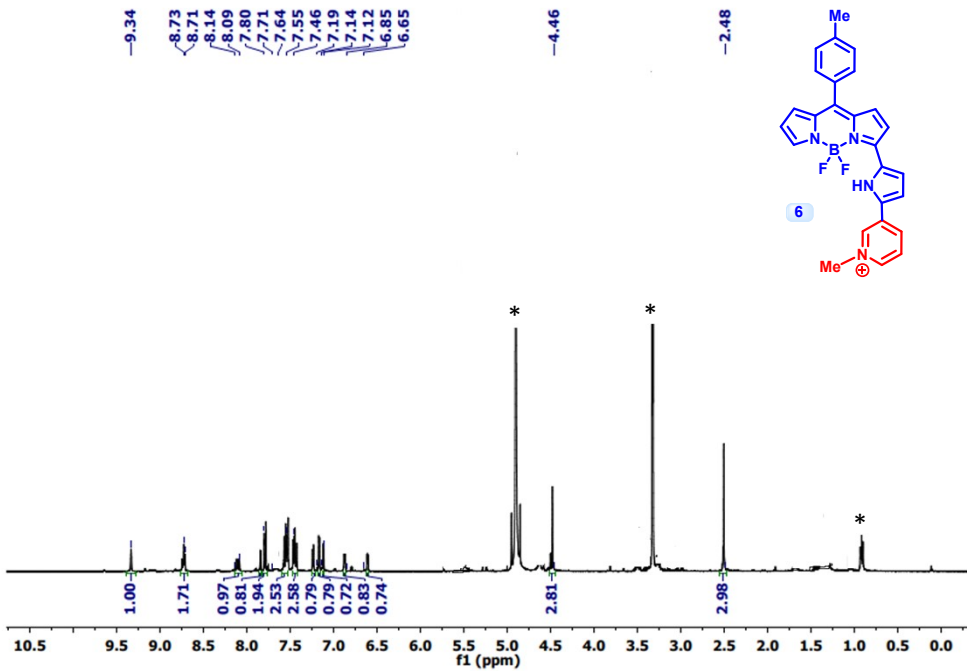
**Fig S8.**  $^1\text{H}$  NMR of compound **3** in  $\text{CDCl}_3$ .



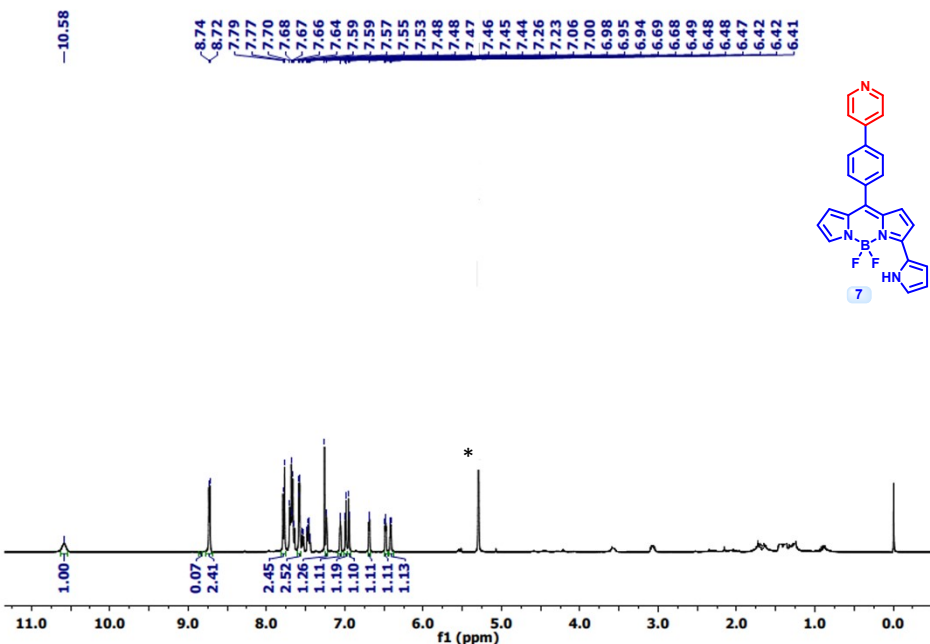
**Fig S9.**  $^1\text{H}$  NMR of compound **4** in  $\text{CDCl}_3$ .



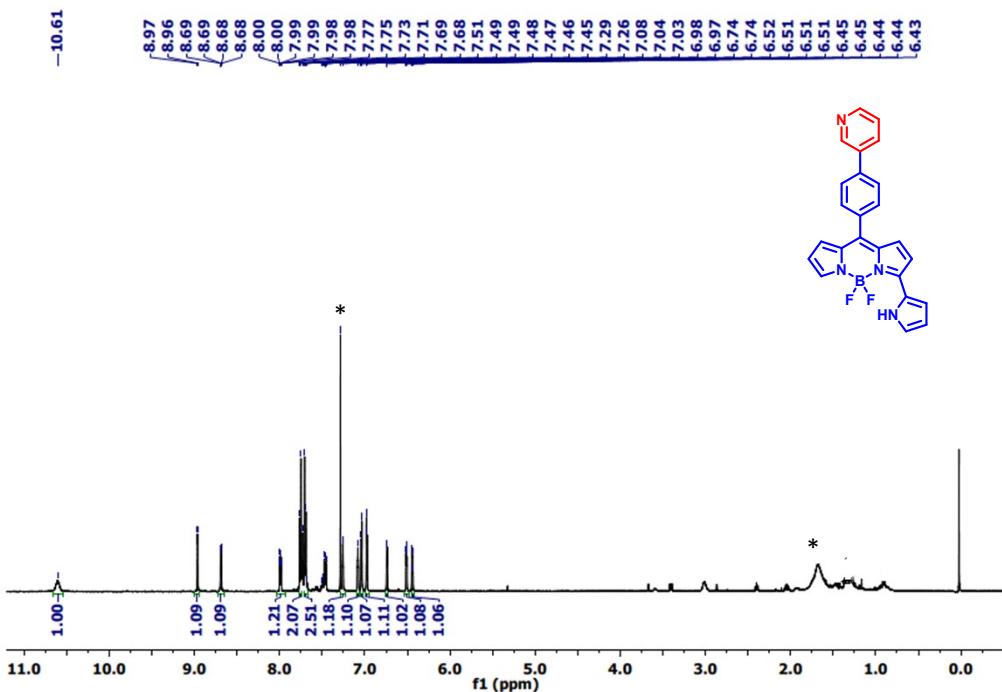
**Fig S10.** <sup>1</sup>H NMR of compound 5 in  $\text{CD}_3\text{OD}$ .



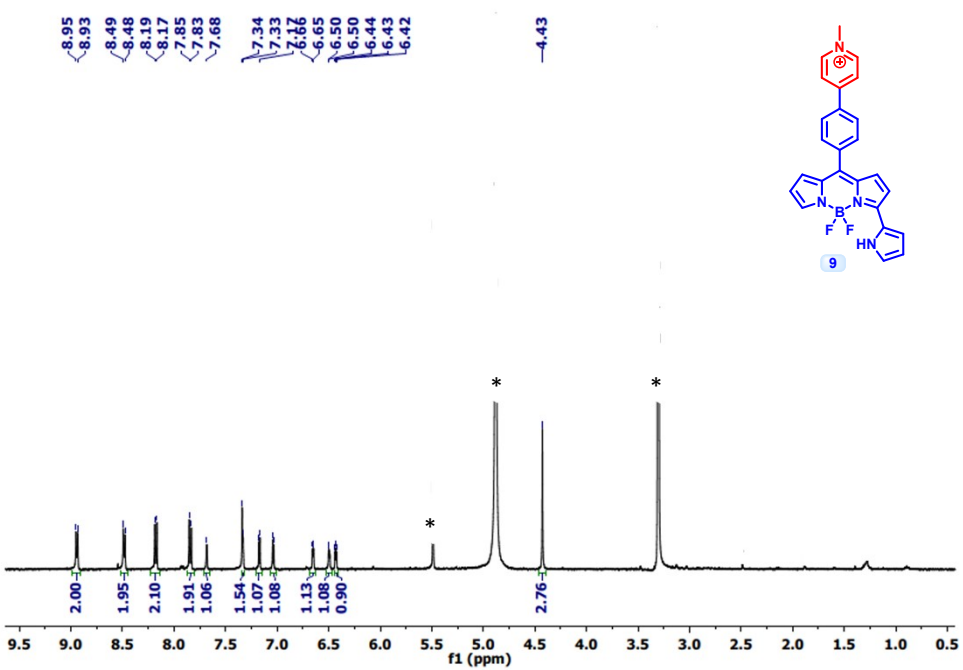
**Fig S11.** <sup>1</sup>H NMR of compound 6 in  $\text{CD}_3\text{OD}$ .



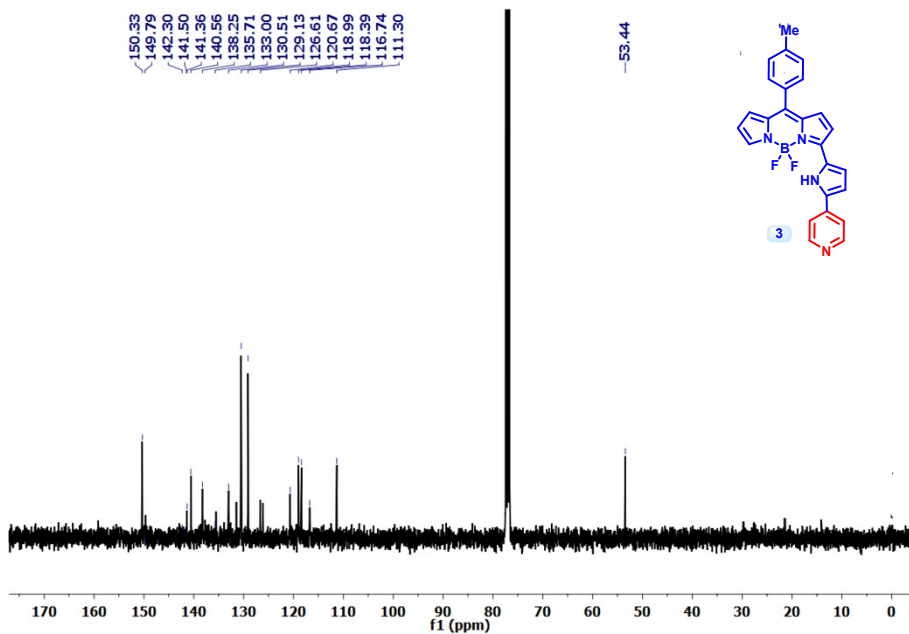
**Fig S12.**  $^1\text{H}$  NMR of compound **7** in  $\text{CDCl}_3$ .



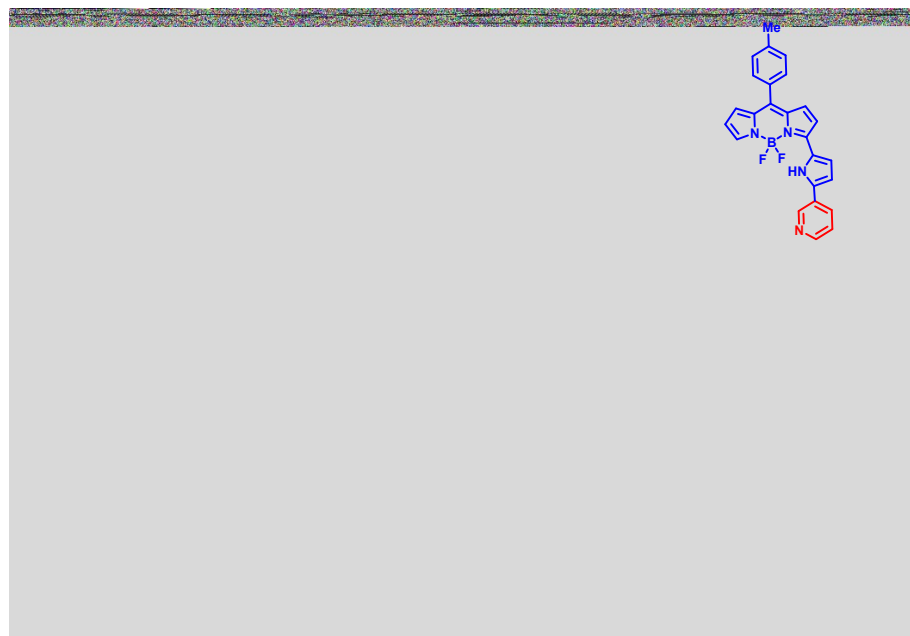
**Fig S13.**  $^1\text{H}$  NMR of compound **8** in  $\text{CDCl}_3$ .



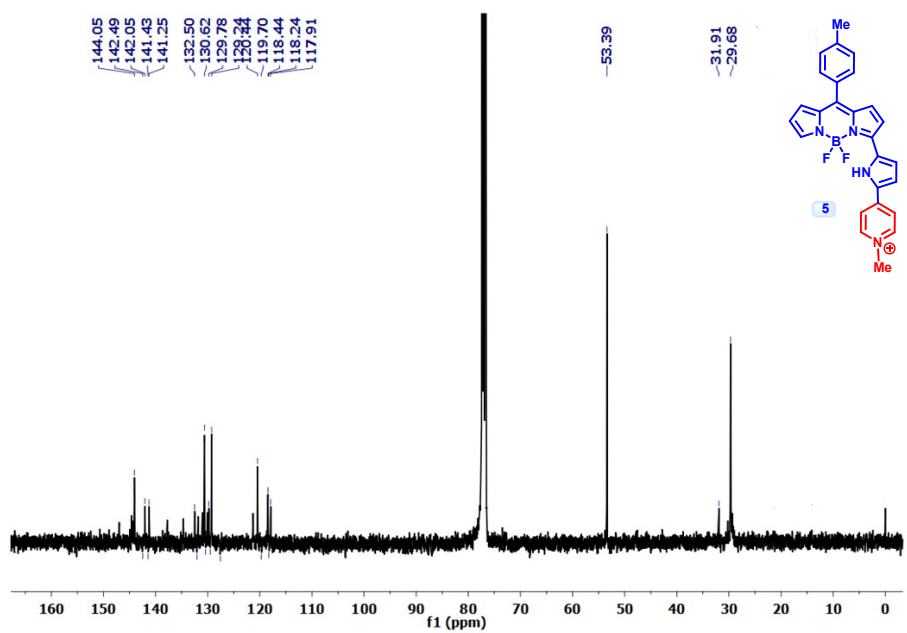
**Fig S14.**  $^1\text{H}$  NMR of compound **9** in  $\text{CD}_3\text{OD}$ .



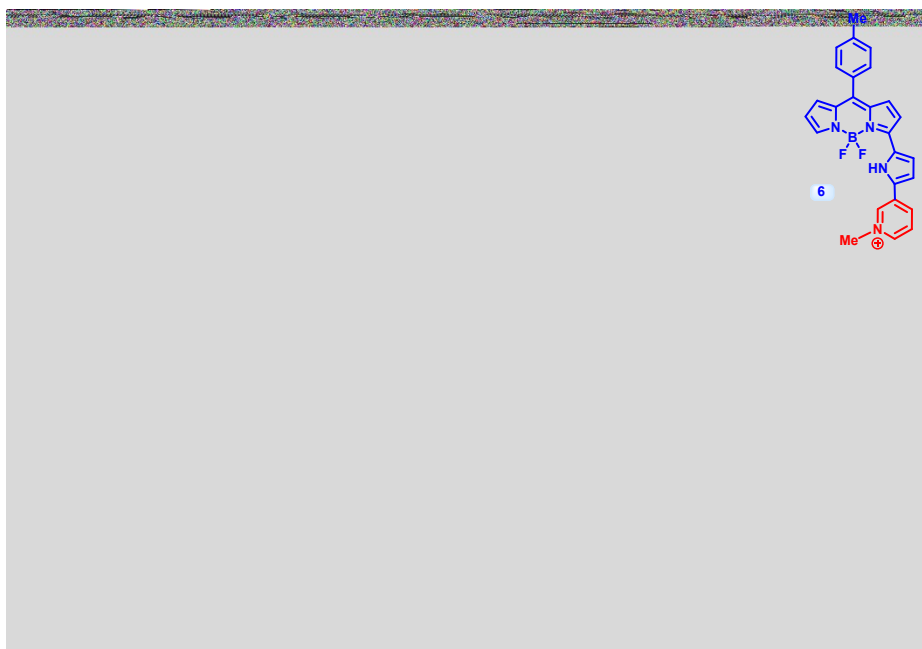
**Fig S15.**  $^{13}\text{C}$  NMR of compound **3** in  $\text{CDCl}_3$ .



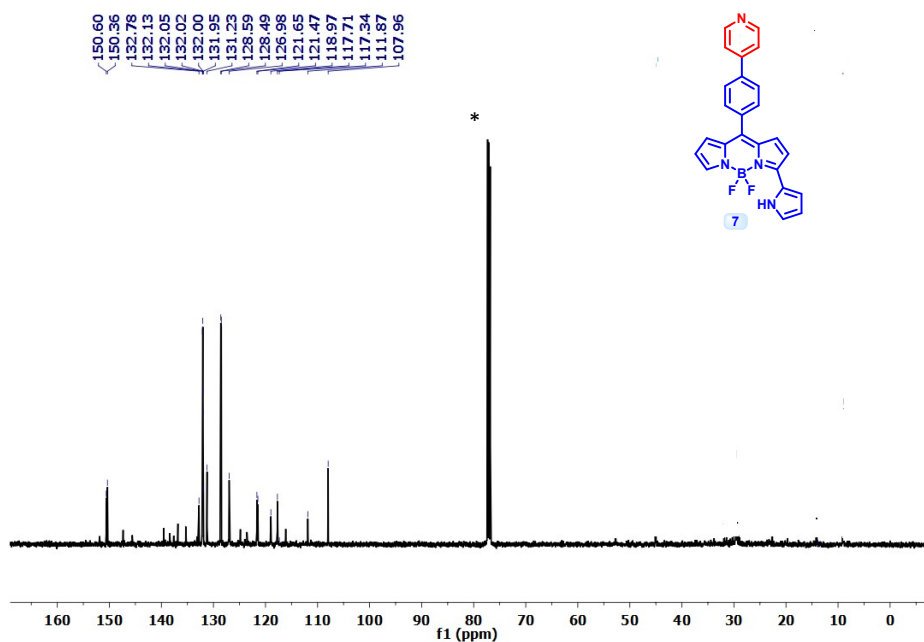
**Fig S16.**  $^{13}\text{C}$  NMR of compound 4 in  $\text{CDCl}_3$ .



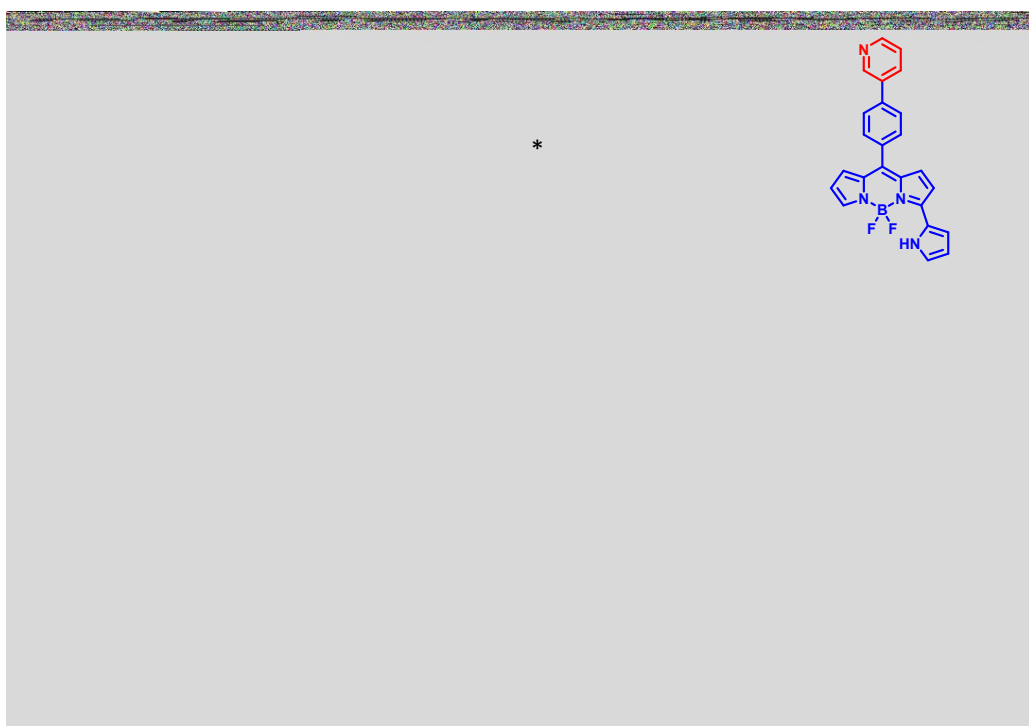
**Fig S17.**  $^{13}\text{C}$  NMR of compound 5 in  $\text{CDCl}_3$ .



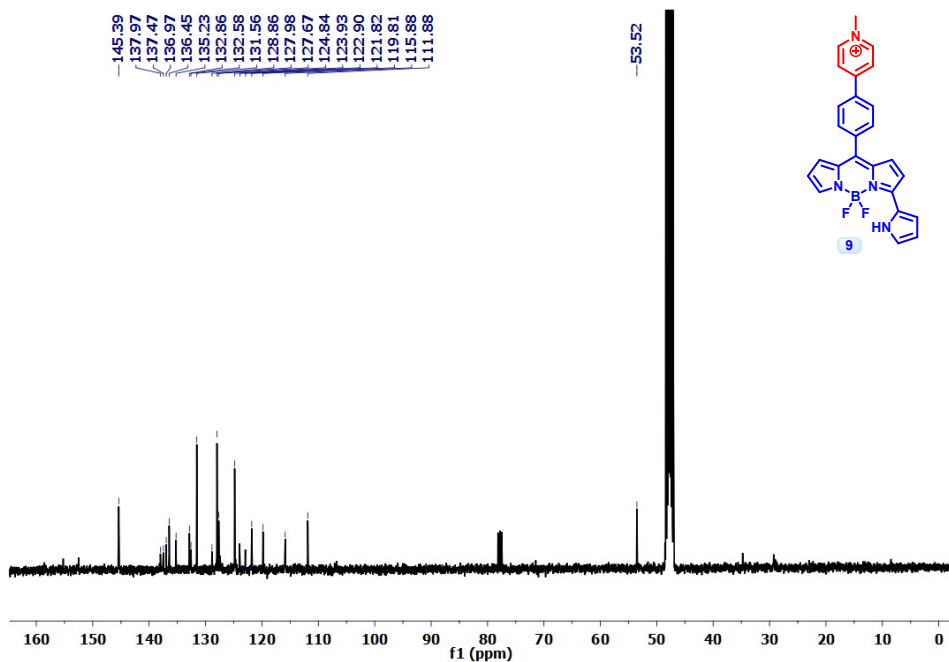
**Fig S18.**  $^{13}\text{C}$  NMR of compound 6 in  $\text{CDCl}_3$ .



**Fig S19.**  $^{13}\text{C}$  NMR of compound 7 in  $\text{CDCl}_3$ .

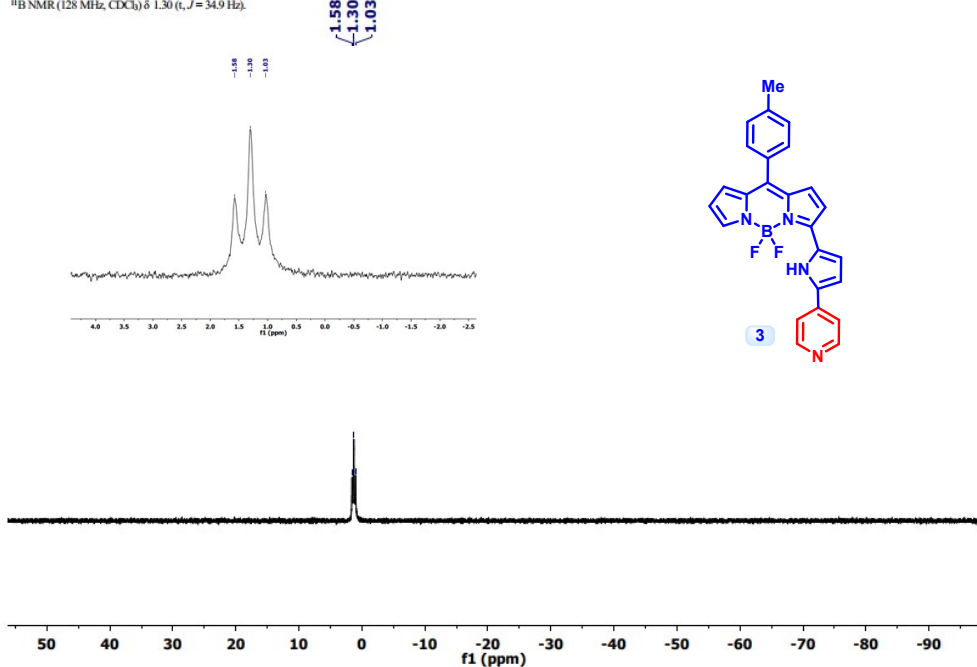


**Fig S20.**  $^{13}\text{C}$  NMR of compound **8** in  $\text{CDCl}_3$ .

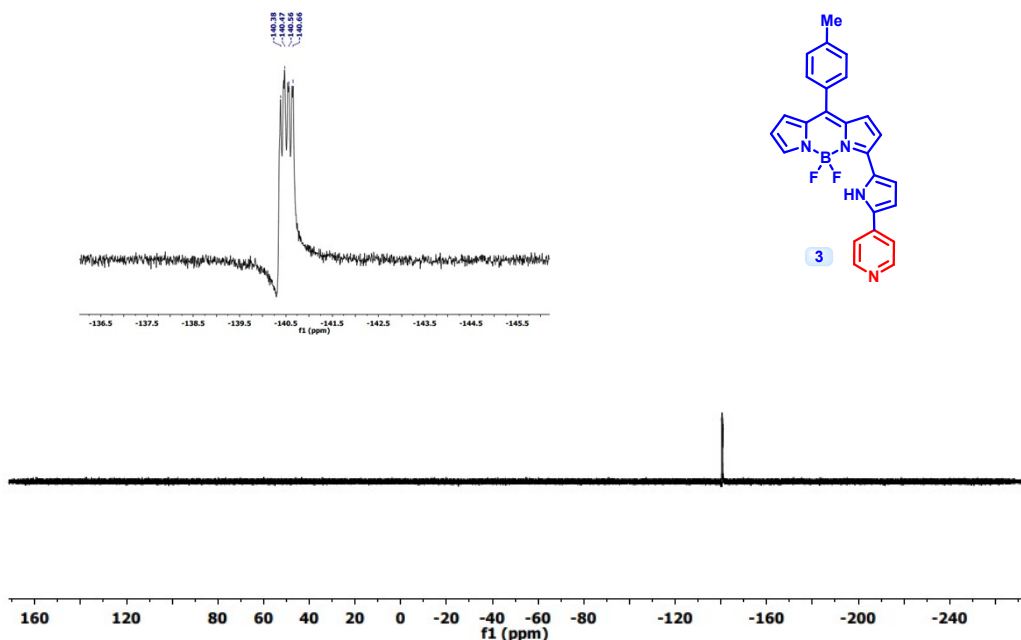


**Fig S21.**  $^{13}\text{C}$  NMR of compound **9** in  $\text{CD}_3\text{OD}$ .

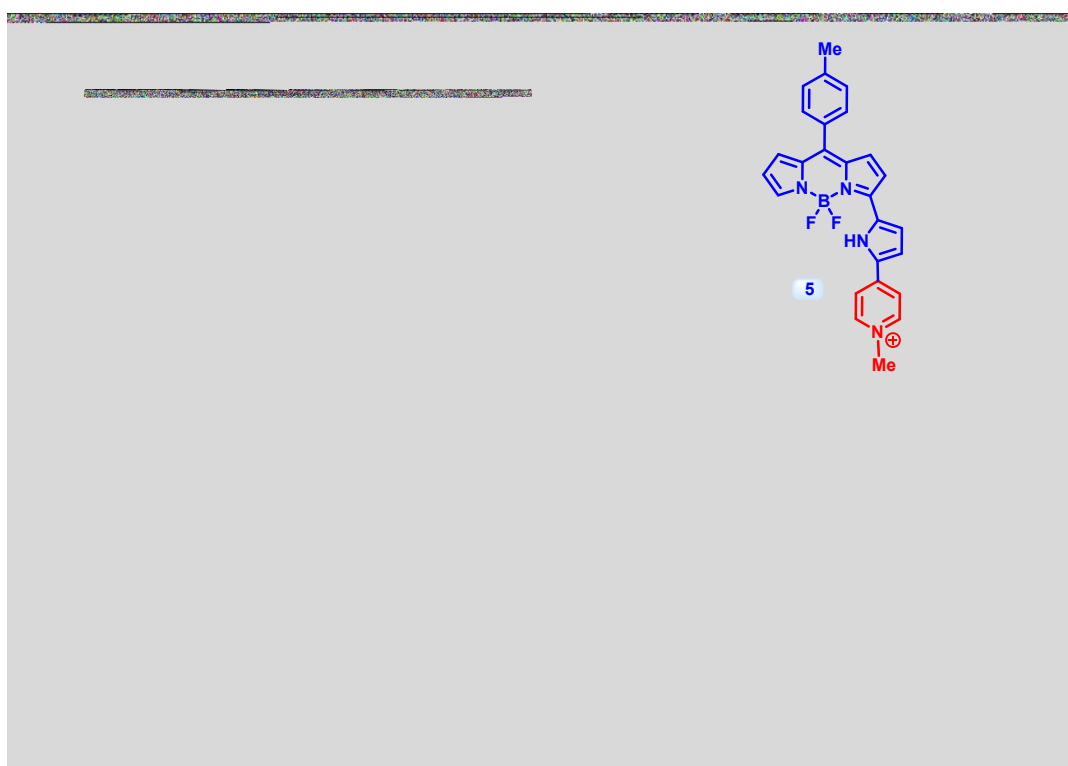
<sup>11</sup>B NMR (128 MHz, CDCl<sub>3</sub>) δ 1.30 (t, *J* = 34.9 Hz).



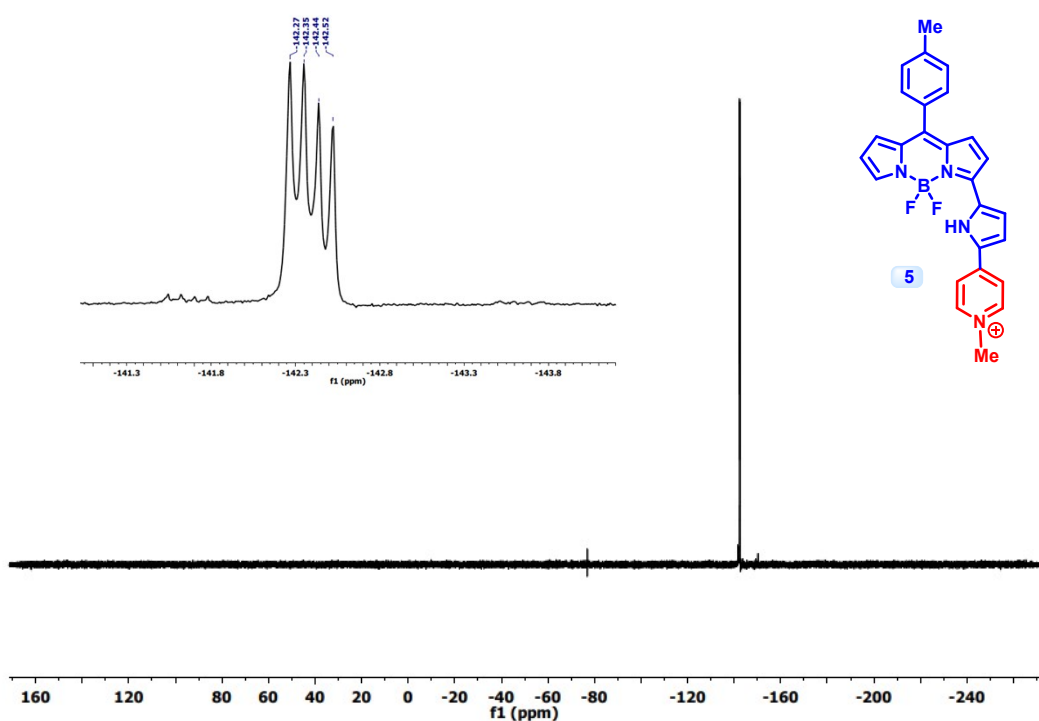
**Fig S22.** <sup>11</sup>B Spectrum of compound 3 in CDCl<sub>3</sub>.



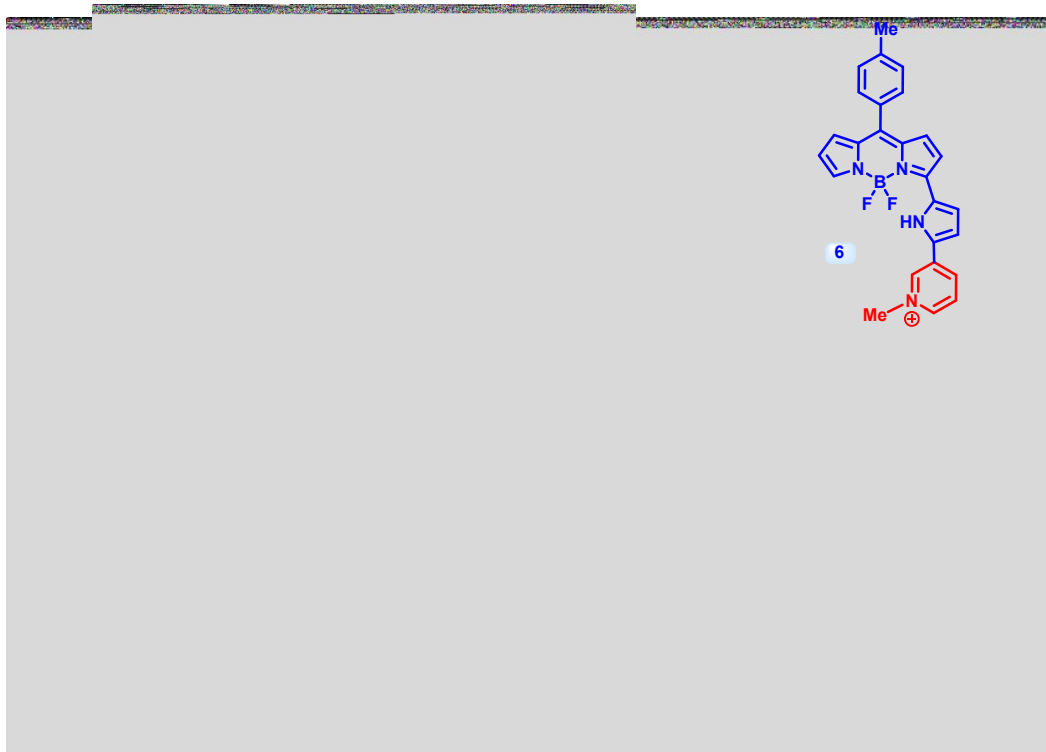
**Fig S23.** <sup>19</sup>F Spectrum of compound 3 in CDCl<sub>3</sub>.



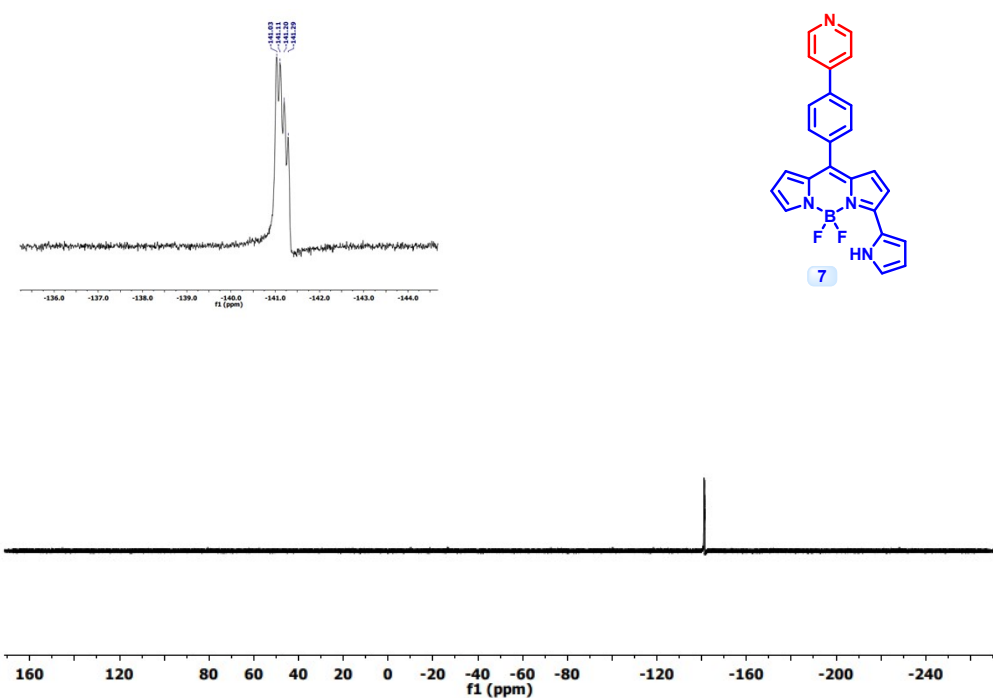
**Fig S24.**  $^{11}\text{B}$  Spectrum of compound **5** in  $\text{CD}_3\text{OD}$ .



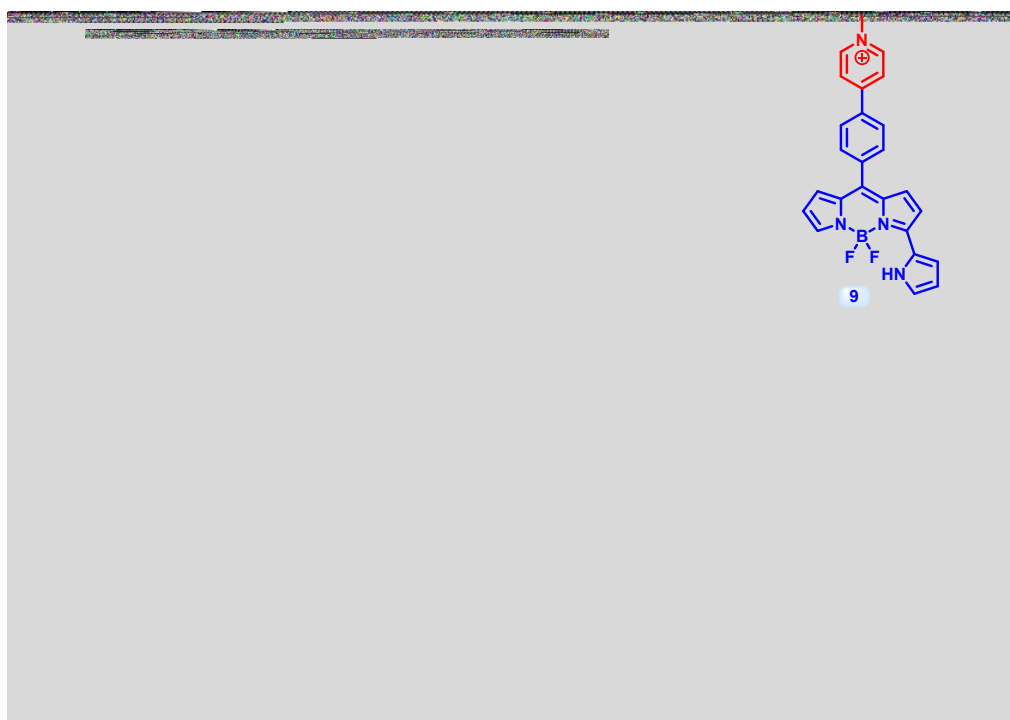
**Fig S25.**  $^{19}\text{F}$  Spectrum of compound **5** in  $\text{CD}_3\text{OD}$ .



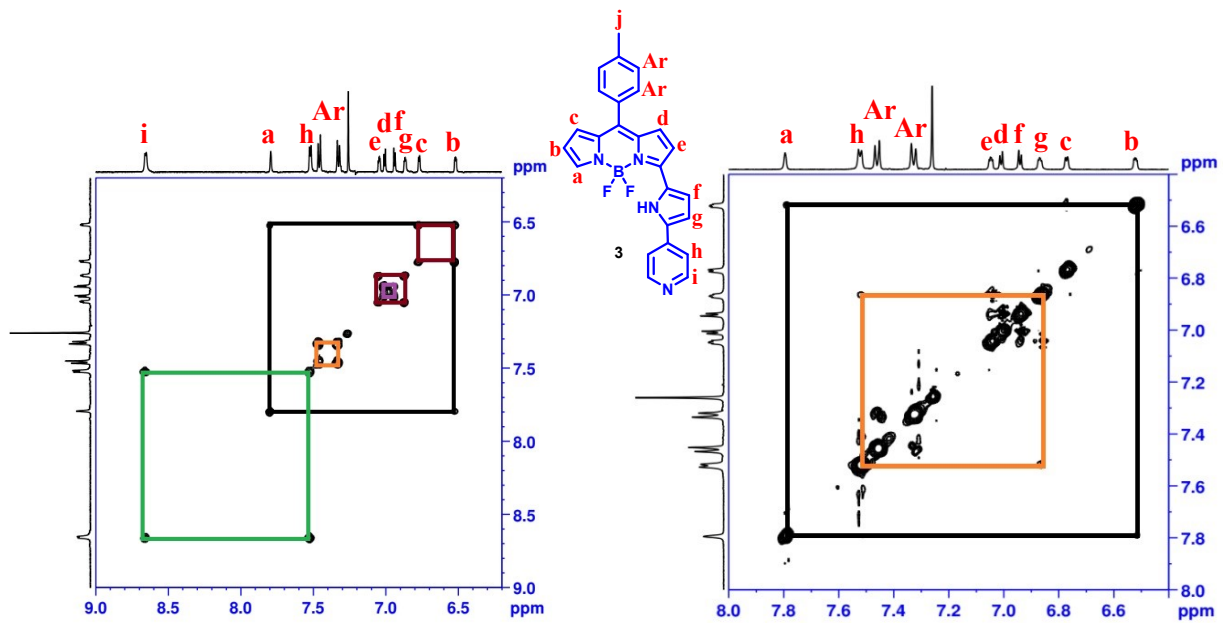
**Fig S26.**  $^{19}\text{F}$  Spectrum of compound 6 in  $\text{CD}_3\text{OD}$ .



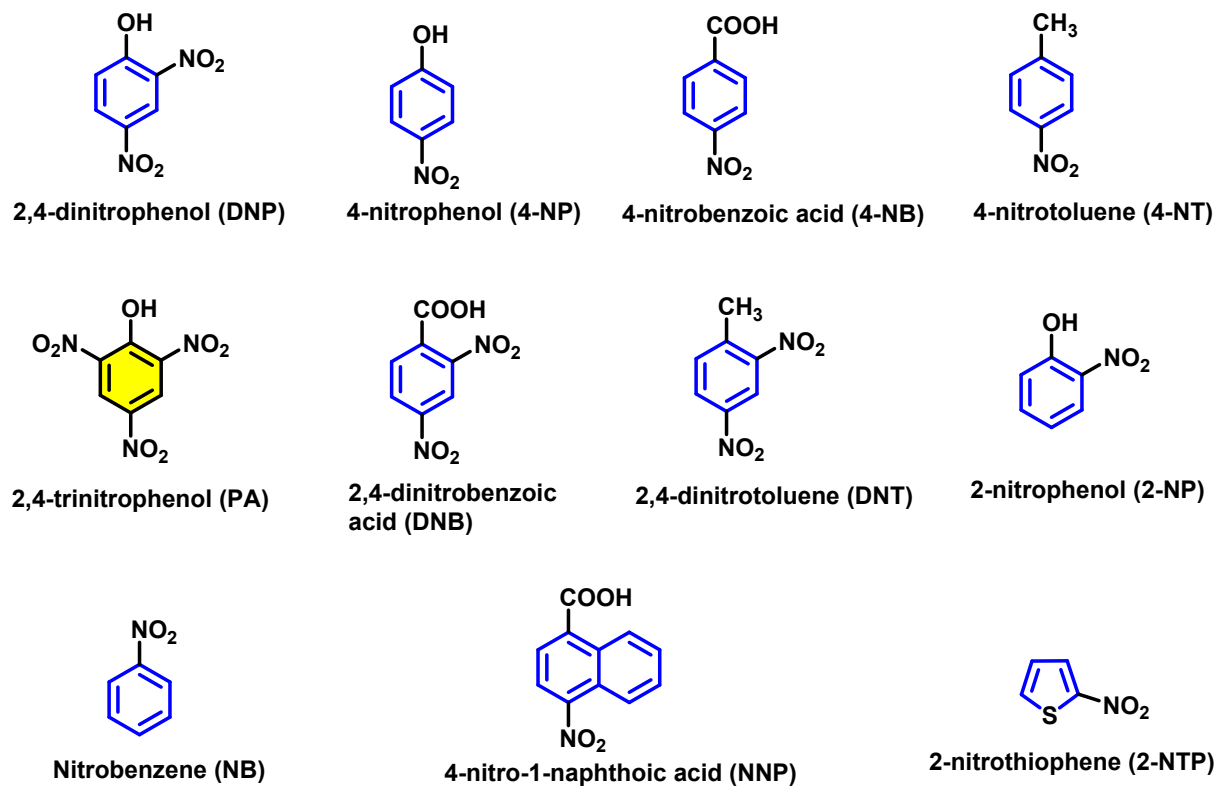
**Fig S27.**  $^{19}\text{F}$  Spectrum of compound 7 in  $\text{CDCl}_3$ .



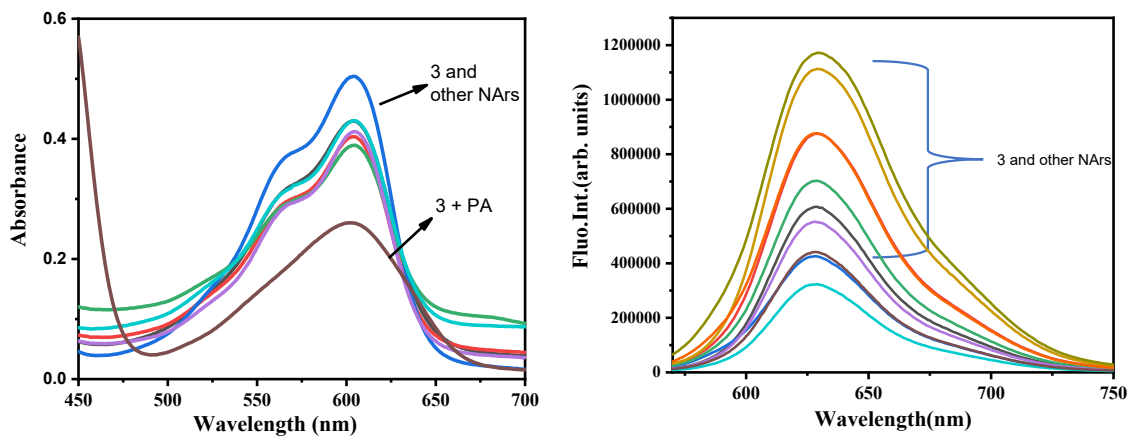
**Fig S28.**  $^{19}\text{F}$  Spectrum of compound **9** in  $\text{CD}_3\text{OD}$ .



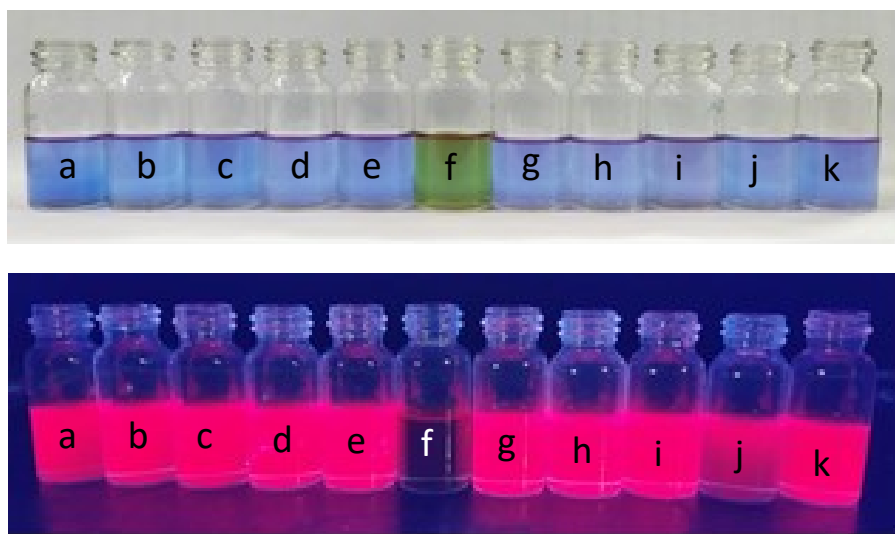
**Fig S29.** COSY and NOESY spectrum of compound **3** in  $\text{CDCl}_3$ .



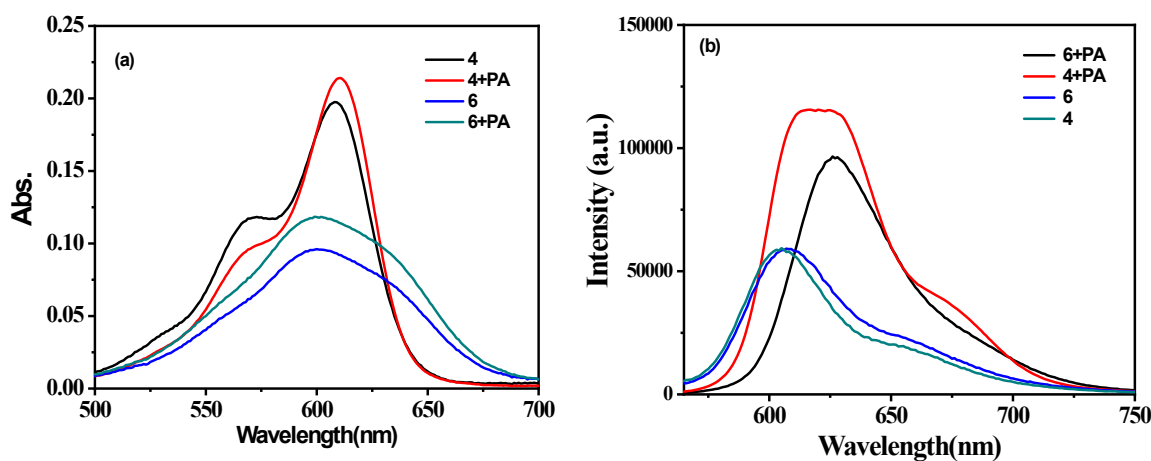
**Fig S30.** Structure of all nitroaromatics studied in this work.



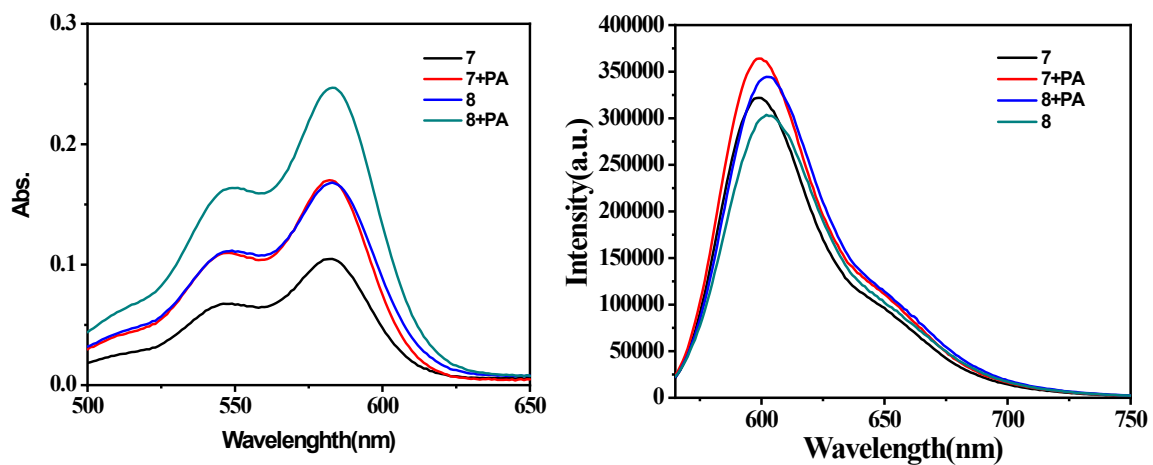
**Fig S31.** UV and Fluorescence spectra of compound 3 in the presence of all nitroaromatics in  $\text{CH}_3\text{OH}$ .



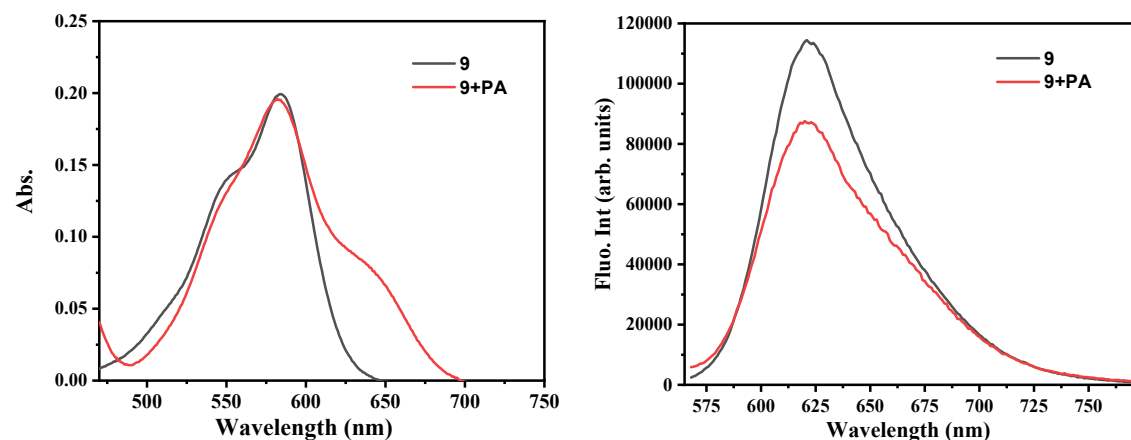
**Fig S32.** Compound **3** in the presence of all nitroaromatics under normal and UV light where a = NB, b = 2-NP, c = 4-NP, d = 4-NT, e = DNT, f = PA, g = NNP, h = NTP, i = DNB, j = DNP and k = 2-NTP.



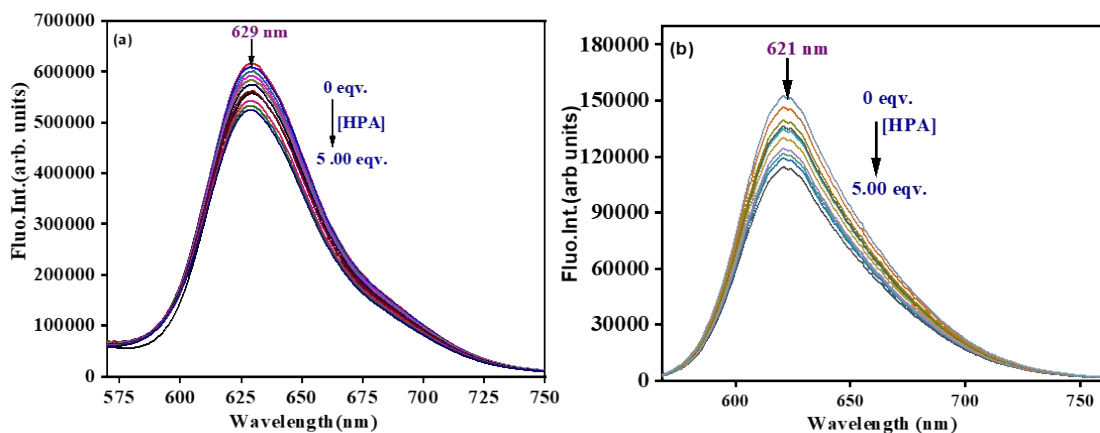
**Fig S33.** UV and Fluorescence spectra of compounds **4** and **6** in the presence of HPA.



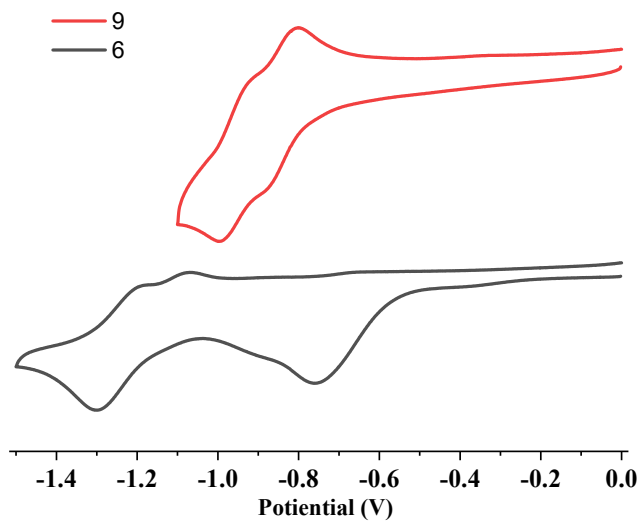
**Fig S34.** UV and Fluorescence spectra of compounds **7** and **8** in the presence of HPA.



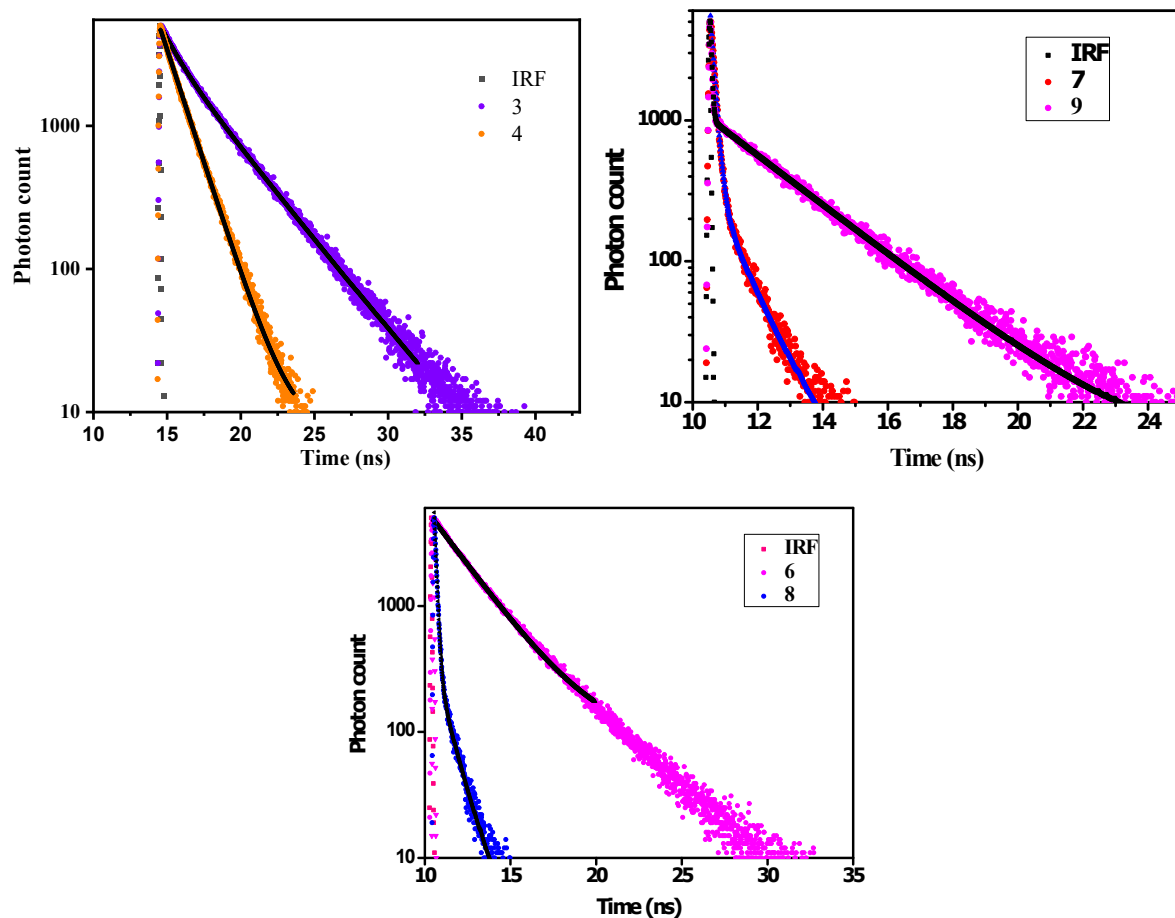
**Fig S35.** UV and Fluorescence spectra of compound **9** in the presence of HPA.



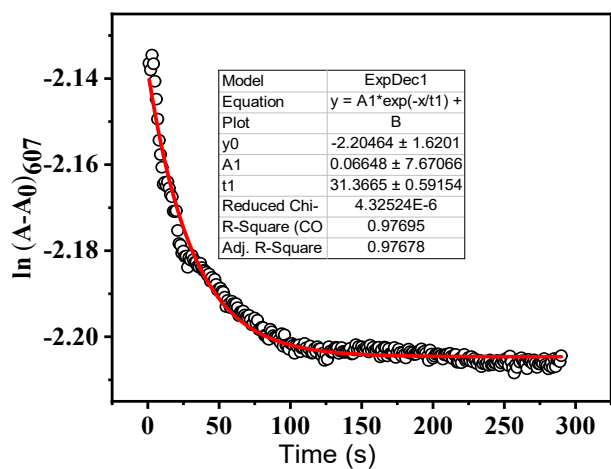
**Fig. S36.** Fluorescence titration of (a) compound **6** and (b) **9** in the presence of HPA.



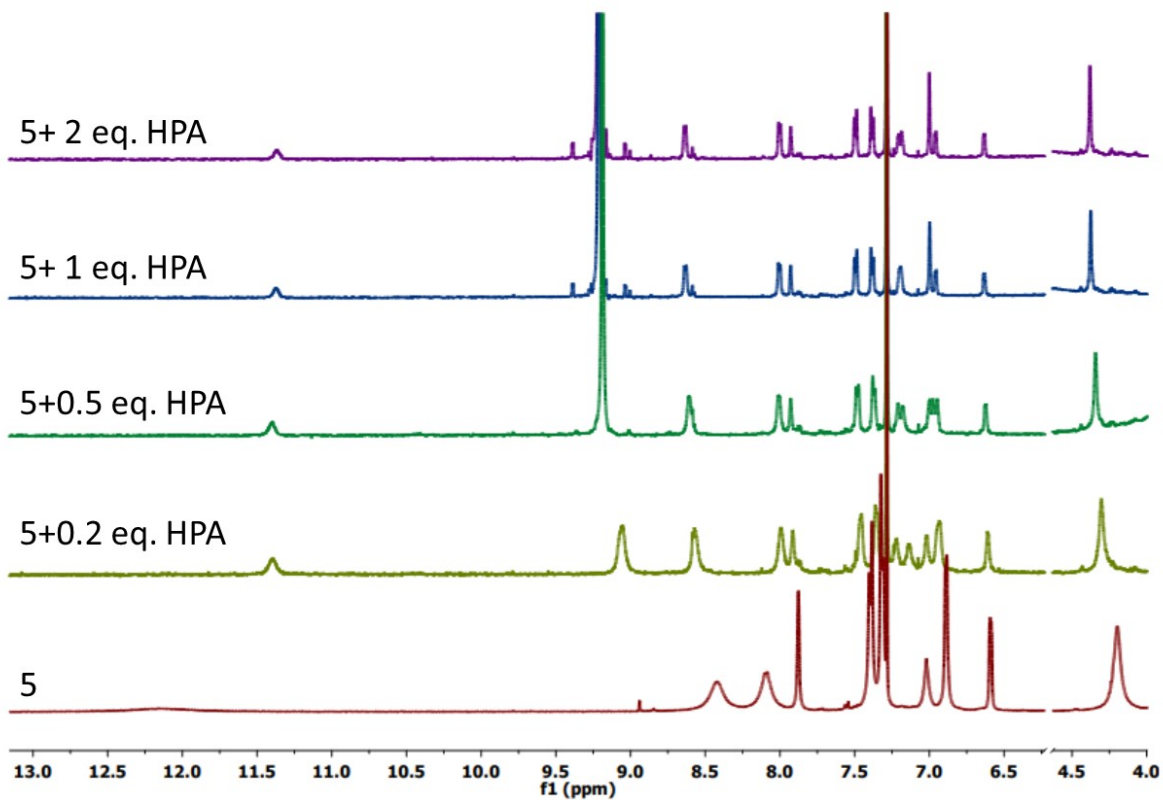
**Fig S37.** Cyclic voltammograms of compounds **6** and **9** recorded at  $50 \text{ mVs}^{-1}$  scan rates in  $\text{CH}_2\text{Cl}_2$  using tetra-butyl ammonium perchlorate (TBAP) as a supporting electrolyte.



**Fig S38.** Decay profile of compounds (a) **3**, **4** (b) **7**, **9** and (c) **6** and **8** with  $\lambda_{\text{ex}} = 580 \text{ nm}$ ,  $\lambda_{\text{em}} = 605 \text{ nm}$ .

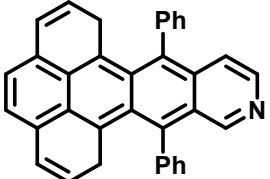
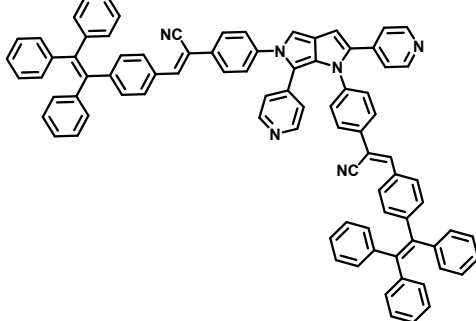
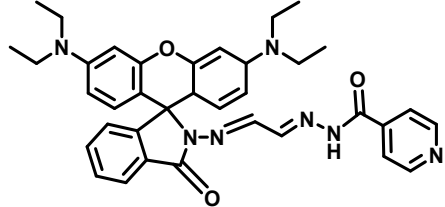
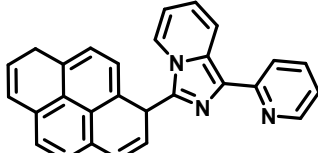
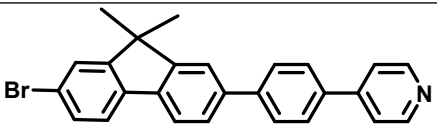
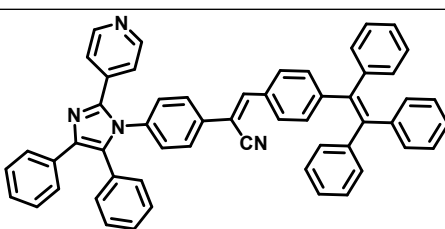


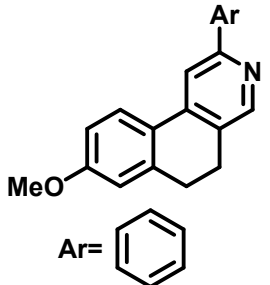
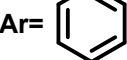
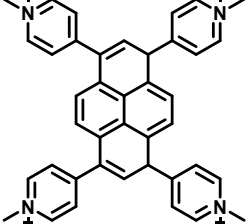
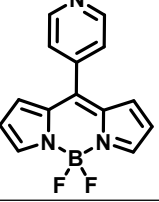
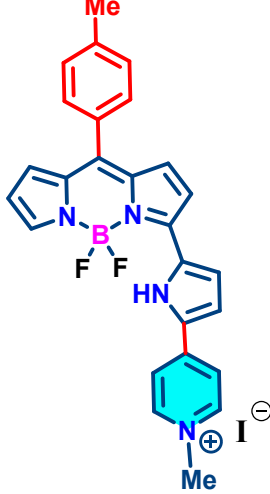
**Fig S39.** Absorbance spectra of compound **5** with the stoichiometric addition of PAH with respect to time(s) for determination of rate constant.



**Fig. S40.**  $^1\text{H}$  NMR of **5** (10mM,  $\text{CDCl}_3\text{-d}_6$ ) on addition of HPA.

**Table-S1:** Comparison of reported molecules for sensing picric acid (PAH) and their sensing parameters with the synthesized molecule in this work.

Compound	Medium	Binding Constant $K_{sv}$	LOD	Reference
	CH <sub>3</sub> CN	-	2.42 μM	[S4]
	DMF/H <sub>2</sub> O	$2.30 \times 10^6 \text{ M}^{-1}$	31.5 nM	[S5]
	CH <sub>3</sub> CN/H <sub>2</sub> O	-	37.3 nM	[S6]
	DMSO	-	63 nM	[S7]
	EtOH/H <sub>2</sub> O	$4.60 \times 10^5 \text{ M}^{-1}$	10 μM	[S8]
	THF/H <sub>2</sub> O	$6.92 \times 10^4 \text{ M}^{-1}$	155 nM	[S9]

 <p><b>Ar</b> = </p>	CH <sub>3</sub> CN	$3.30 \times 10^5 \text{ M}^{-1}$	-	[S10]
	H <sub>2</sub> O	$6.04 \times 10^4 \text{ M}^{-1}$	-	[S11]
	DMSO/H <sub>2</sub> O	$7.69 \times 10^4 \text{ M}^{-1}$	13.06 nM	[S12]
	H <sub>2</sub> O/MeOH 9:1	$4.94 \times 10^7 \text{ M}^{-1}$	7.90 pM	<b>This Work</b>

- Not reported in the paper

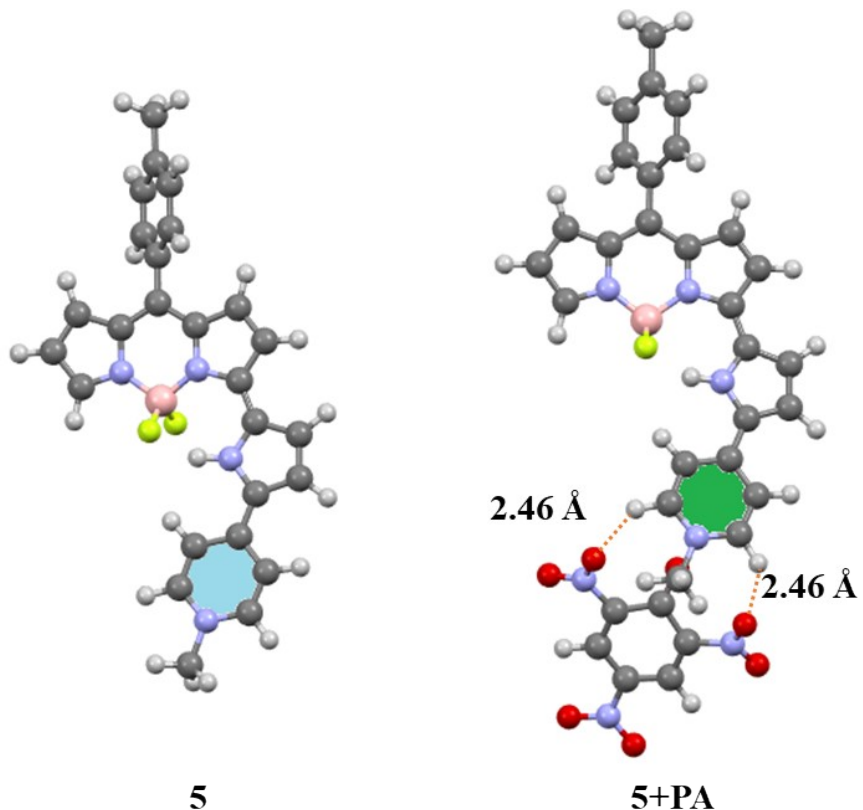


**Fig. S41:** Ground state optimized structure of compound **5** and **5+PA**.

**Table-S2.**  $S_0$  optimized geometry of compound **5** using B3LYP/6-31G (d,p) level of theory.

Atom	X	Y	Z	Atom	X	Y	Z
C	-6.620803000	0.234411000	0.750068000	C	-5.263823000	0.536817000	0.823611000
C	-4.353775000	-0.014820000	-0.095223000	C	-4.854845000	-0.874746000	-1.088589000
C	-6.213512000	-1.168960000	-1.155615000	C	-7.123687000	-0.620232000	-0.240482000
C	-8.598741000	-0.920280000	-0.336575000	C	-2.912862000	0.313527000	-0.018423000
C	-2.476111000	1.653726000	0.013686000	N	-1.132156000	1.970217000	0.155925000
B	0.020526000	0.971746000	0.342651000	N	-0.576909000	-0.447602000	0.074012000
C	-1.931980000	-0.703097000	0.032785000	C	0.082173000	-1.673798000	0.158730000
C	-0.912545000	-2.720552000	0.178664000	C	-2.136175000	-2.135300000	0.096230000
C	-3.202673000	2.879866000	-0.125883000	C	-2.282772000	3.910969000	-0.055804000
C	-1.012477000	3.319074000	0.115014000	F	0.576286000	1.031914000	1.604767000
F	1.036902000	1.276945000	-0.611552000	C	1.460311000	-1.884919000	0.178424000
N	2.420957000	-0.909257000	0.011073000	C	3.675382000	-1.447817000	0.087599000
C	3.511967000	-2.849755000	0.329960000	C	2.166426000	-3.118494000	0.379112000

C	4.861697000	-0.674223000	-0.049502000	C	4.832562000	0.743349000	-0.227756000
C	5.991618000	1.455931000	-0.358161000	N	7.218671000	0.846735000	-0.328568000
C	7.284554000	-0.512764000	-0.152401000	C	6.155935000	-1.271358000	-0.017522000
H	-7.300579000	0.662399000	1.481755000	H	-4.898673000	1.181628000	1.617119000
H	-4.179058000	-1.292013000	-1.829397000	H	-6.576241000	-1.829334000	-1.938678000
H	-9.089706000	-0.833485000	0.636399000	H	-9.096323000	-0.218698000	-1.017304000
				H	-0.695872000	-3.777818000	0.229211000
H	-3.101728000	-2.616582000	0.088877000	H	-4.268567000	2.952657000	-0.279229000
H	-2.476370000	4.971203000	-0.130674000	H	-0.043675000	3.790471000	0.199183000
H	2.171316000	0.041838000	-0.259440000	H	4.311867000	-3.562734000	0.465320000
H	1.705663000	-4.077463000	0.565091000	H	3.896938000	1.289626000	-0.257568000
H	5.997910000	2.530729000	-0.489956000	H	8.278538000	-0.941659000	-0.131705000
H	6.272137000	-2.340699000	0.107626000	C	8.450316000	1.644381000	-0.403333000
H	8.788398000	1.923418000	0.599153000	H	8.261983000	2.546518000	-0.985877000
H	9.228575000	1.063174000	-0.899339000				

**Table-S3.** S<sub>0</sub> optimized geometry of the compound **5+PA** using B3LYP/6-31G (d,p) level of theory.

Atom	X	Y	Z	Atom	X	Y	Z
C	-9.550186000	-1.695362000	-1.335923000	C	-8.178475000	-1.655874000	-1.098945000
C	-7.604434000	-0.619567000	-0.341221000	C	-8.462846000	0.372143000	0.165672000
C	-9.833090000	0.327910000	-0.078781000	C	-10.405288000	-0.707082000	-0.830557000
C	-11.895019000	-0.769653000	-1.065425000	C	-6.147427000	-0.584091000	-0.083339000
C	-5.473120000	-1.703647000	0.447245000	N	-4.099686000	-1.695371000	0.630356000
B	-3.143304000	-0.555066000	0.269942000	N	-4.032352000	0.668333000	-0.122933000
C	-5.378913000	0.577724000	-0.375133000	C	-3.596104000	1.921667000	-0.576965000
C	-4.722245000	2.611293000	-1.130483000	C	-5.816133000	1.802814000	-1.003440000
C	-5.966651000	-2.963125000	0.916929000	C	-4.873813000	-3.691897000	1.365407000
C	-3.735704000	-2.887055000	1.180040000	F	-2.353435000	-0.247188000	1.423132000
F	-2.286194000	-0.880924000	-0.763839000	C	-2.299757000	2.446048000	-0.463592000
N	-1.271259000	1.867208000	0.236674000	C	-0.139049000	2.634328000	0.158262000
C	-0.456808000	3.762858000	-0.645457000	C	-1.779030000	3.655966000	-1.025543000

C	1.090043000	2.266769000	0.801634000	C	1.241747000	1.031479000	1.478787000
C	2.432214000	0.716850000	2.089804000	N	3.475387000	1.581215000	2.083863000
C	3.384003000	2.751257000	1.405089000	C	2.219164000	3.118570000	0.776566000
H	-9.962615000	-2.503163000	-1.935242000	H	-7.536742000	-2.421230000	-1.524497000
H	-8.053416000	1.173028000	0.774376000	H	-10.471583000	1.106685000	0.330781000
H	-12.130450000	-1.258678000	-2.015175000	H	-12.396109000	-1.340022000	-0.273294000
H	-12.341554000	0.228883000	-1.077770000	H	-4.692436000	3.608481000	-1.546085000
H	-6.828303000	2.004430000	-1.317166000	H	-7.005715000	-3.255030000	0.927181000
H	-4.877766000	-4.685270000	1.790694000	H	-2.700898000	-3.093073000	1.412580000
H	-1.418505000	1.038131000	0.813466000	H	0.228934000	4.549062000	-0.925540000
H	-2.328165000	4.335512000	-1.660200000	H	0.446199000	0.296366000	1.505657000
H	2.605510000	-0.236703000	2.569521000	H	4.282314000	3.351759000	1.365885000
H	2.195608000	4.065245000	0.252000000	C	4.734492000	1.222042000	2.763270000
H	4.837133000	0.138396000	2.735212000	H	5.557378000	1.674487000	2.211980000
H	4.704459000	1.587472000	3.793936000	O	4.558859000	0.354911000	-0.003905000
C	5.647207000	-0.208829000	-0.184654000	C	6.843553000	0.465225000	-0.706178000
C	5.874329000	-1.644522000	0.026194000	C	7.956940000	-0.206407000	-1.166331000
C	6.988804000	-2.314546000	-0.433673000	C	8.022517000	-1.597279000	-1.042883000
H	8.785343000	0.338717000	-1.600111000	H	7.075145000	-3.385873000	-0.305976000
N	4.883029000	-2.425191000	0.741827000	O	4.210314000	-1.863697000	1.622403000
O	4.775947000	-3.624828000	0.477976000	N	6.875581000	1.914075000	-0.762907000
O	7.561681000	2.454601000	-1.633349000	O	6.243550000	2.553974000	0.094163000
N	9.200826000	-2.299266000	-1.505875000	O	10.105382000	-1.633997000	-2.022828000
O	9.238418000	-3.526259000	-1.360814000				

**Table-S4.** Major transitions were calculated using TD-DFT studies of **5**.

No.	Wavelength (nm)	Osc. Strength	Major contributions
1	585.51	1.0736	HOMO->LUMO (100%)
2	496.68	0.0015	HOMO->L+1 (100%)
3	462.53	0.0089	H-1->LUMO (98%)
4	440.75	0.0076	HOMO->L+2 (98%)

5	419.40	0.0104	H-2->LUMO (47%), HOMO->L+3 (50%)
6	414.09	0.141	H-1->L+1 (97%)
7	400.54	0.4218	H-4->LUMO (19%), H-2->LUMO (42%), HOMO->L+3 (31%)
8	391.76	0.011	HOMO->L+4 (86%)
9	390.32	0.0005	H-3->LUMO (93%)
10	388.93	0.0007	H-3->L+1 (85%)
11	373.43	0.0122	H-5->LUMO (94%)
12	367.01	0.0861	H-6->LUMO (60%), H-4->LUMO (31%)
13	363.54	0.1597	H-1->L+2 (80%), H-1->L+4 (12%)
14	347.22	0.0148	H-3->L+2 (22%), H-3->L+4 (61%)
15	342.29	0.1606	H-4->LUMO (11%), H-1->L+3 (69%)
16	338.55	0.3303	H-6->LUMO (19%), H-4->LUMO (30%), H-1->L+3 (25%), HOMO->L+3 (10%)
17	337.00	0.0189	H-7->LUMO (88%)
18	335.75	0.0001	H-3->L+2 (66%), H-3->L+4 (26%)
19	331.06	0.0025	H-11->L+4 (10%), H-9->L+1 (39%), H-8->L+1 (14%)
20	328.39	0.0003	H-2->L+1 (92%)
21	325.09	0.0949	HOMO->L+5 (81%)
22	322.79	0.0017	H-11->L+1 (42%), H-9->L+2 (12%), H-9->L+4 (10%)
23	322.67	0.029	H-9->LUMO (18%), H-8->LUMO (57%), H-7->LUMO (10%), HOMO->L+5 (11%)
24	314.15	0.1458	H-1->L+2 (10%), H-1->L+4 (75%)
25	310.85	0.0	H-10->L+2 (79%), H-10->L+4 (11%)
26	305.00	0.0034	H-2->L+2 (89%)
27	304.76	0.0002	H-9->LUMO (75%), H-8->LUMO (23%)
28	302.41	0.0001	H-3->L+3 (91%)
29	298.56	0.0018	H-2->L+3 (87%)
30	298.05	0.0	H-4->L+1 (93%)

31	289.68	0.0	H-5->L+1 (90%)
32	283.52	0.0	H-6->L+1 (91%)
33	279.75	0.0241	H-4->L+2 (42%), H-4->L+3 (12%), HOMO->L+6 (26%)
34	278.75	0.0031	H-2->L+4 (69%), HOMO->L+6 (14%)
35	277.90	0.0026	H-11->LUMO (75%)
36	277.75	0.0013	H-20->L+1 (12%), H-15->L+2 (10%), H-11->LUMO (11%), H-10->L+1 (11%), H-2->L+4 (16%)
37	276.78	0.0029	H-4->L+2 (41%), HOMO->L+6 (27%)
38	275.82	0.0033	H-19->L+1 (23%), H-15->L+1 (14%), H-11->L+1 (16%), H-9->L+2 (13%)
39	274.36	0.0182	H-12->LUMO (56%), H-10->LUMO (11%), H-1->L+5 (27%)
40	274.12	0.0004	H-7->L+1 (79%)
41	273.25	0.0003	H-19->L+2 (18%), H-15->L+2 (35%), H-10->L+1 (10%)
42	272.75	0.0004	H-5->L+2 (65%), H-5->L+3 (21%)
43	272.69	0.0001	H-10->LUMO (76%), H-1->L+5 (22%)
44	272.30	0.1017	H-4->L+3 (40%), HOMO->L+7 (34%), HOMO->L+8 (10%)
45	271.64	0.0064	H-12->LUMO (34%), H-10->LUMO (11%), H-1->L+5 (50%)
46	271.34	0.0093	H-4->L+3 (17%), HOMO->L+7 (59%)
47	268.43	0.0011	H-6->L+3 (16%), H-5->L+2 (27%), H-5->L+3 (47%)
48	267.45	0.0	H-9->L+2 (46%), H-8->L+2 (16%)
49	266.99	0.007	H-6->L+2 (69%), H-6->L+3 (11%), H-5->L+3 (13%)
50	265.59	0.0001	H-9->L+1 (22%), H-8->L+1 (66%), H-7->L+1 (10%)

**Table-S5.** Major transitions were calculated using TD-DFT studies of **5+PA**.

No.	Wavelength (nm)	Osc. Strength	Major contributions
1	1194.44	0.0508	HOMO(A)->LUMO(A) (57%), HOMO(B)->LUMO(B) (35%)
2	884.14	0.1705	HOMO(A)->LUMO(A) (27%), HOMO(B)->LUMO(B) (62%)
3	730.51	0.0037	H-3(B)->LUMO(B) (69%), H-2(B)->LUMO(B) (23%)
4	646.62	0.5647	HOMO(A)->LUMO(A) (12%), H-1(B)->LUMO(B) (80%)
5	627.98	0.1564	H-3(B)->LUMO(B) (24%), H-2(B)->LUMO(B) (71%)
6	618.86	0.0053	H-4(B)->LUMO(B) (88%)
7	541.64	0.0352	HOMO(A)->L+1(A) (93%)
8	528.24	0.0126	H-5(B)->LUMO(B) (92%)
9	486.07	0.017	H-1(A)->LUMO(A) (49%), H-6(B)->LUMO(B) (24%), HOMO(B)->L+1(B) (13%)
10	452.29	0.095	H-1(A)->LUMO(A) (11%), HOMO(A)->L+2(A) (63%), H-6(B)->LUMO(B) (12%)
11	445.29	0.1676	HOMO(A)->L+2(A) (11%), H-6(B)->LUMO(B) (12%), HOMO(B)->L+1(B) (57%)
12	415.93	0.1495	H-1(A)->LUMO(A) (13%), H-6(B)->LUMO(B) (39%)
13	380.42	0.0111	H-7(B)->LUMO(B) (92%)
14	375.43	0.1868	HOMO(A)->L+4(A) (63%)
15	367.85	0.0014	HOMO(A)->L+3(A) (75%), H-2(B)->L+1(B) (14%)
16	365.08	0.0071	H-3(B)->L+1(B) (53%), H-2(B)->L+1(B) (15%)
17	354.93	0.025	H-1(B)->L+1(B) (64%)
18	348.63	0.0799	H-2(A)->LUMO(A) (44%), HOMO(B)->L+2(B) (22%)
19	346.79	0.0036	H-3(B)->L+1(B) (21%), H-2(B)->L+1(B) (56%)
20	337.60	0.0453	H-2(A)->LUMO(A) (39%), HOMO(B)->L+2(B) (13%)
21	326.96	0.0921	H-8(B)->LUMO(B) (16%), HOMO(B)->L+2(B) (33%)
22	323.39	0.0064	H-4(B)->L+1(B) (80%)

23	320.07	0.004	H-1(A)->L+1(A) (79%)
24	314.67	0.0113	H-7(A)->LUMO(A) (13%), H-5(B)->L+1(B) (33%)
25	313.13	0.0582	HOMO(A)->L+5(A) (18%), H-8(B)->LUMO(B) (11%)
26	311.10	0.0052	H-3(A)->LUMO(A) (87%)
27	304.96	0.1109	H-4(A)->LUMO(A) (12%), HOMO(A)->L+5(A) (24%), H-5(B)->L+1(B) (11%)
28	299.52	0.0074	H-4(A)->LUMO(A) (50%)
29	298.15	0.0194	H-11(B)->LUMO(B) (45%), H-9(B)->LUMO(B) (37%)
30	295.29	0.0648	H-5(A)->LUMO(A) (20%), HOMO(A)->L+5(A) (10%), H-8(B)->LUMO(B) (17%)
31	294.71	0.0044	HOMO(A)->L+6(A) (44%), H-1(B)->L+2(B) (10%)
32	289.34	0.0053	H-1(A)->L+2(A) (10%), H-11(B)->LUMO(B) (26%), H-9(B)->LUMO(B) (30%)
33	287.70	0.0192	H-6(A)->LUMO(A) (24%), H-1(A)->L+2(A) (10%), H-5(B)->L+1(B) (19%)
34	287.07	0.0241	H-1(A)->L+2(A) (19%), H-11(B)->LUMO(B) (13%), H-9(B)->LUMO(B) (19%), H-1(B)->L+2(B) (10%)
35	282.14	0.0022	H-10(B)->LUMO(B) (94%)
36	281.12	0.0061	H-8(A)->LUMO(A) (16%), H-7(B)->L+1(B) (28%)
37	280.85	0.0049	H-2(B)->L+2(B) (53%)
38	279.82	0.0052	H-7(A)->LUMO(A) (11%), H-7(B)->L+1(B) (15%)
39	277.81	0.009	H-7(A)->LUMO(A) (20%), H-1(A)->L+2(A) (14%), H-6(B)->L+1(B) (17%)
40	277.15	0.0132	H-3(B)->L+2(B) (53%), H-2(B)->L+2(B) (14%)
41	273.79	0.0418	H-8(A)->L+1(A) (14%), HOMO(A)->L+6(A) (17%), H-7(B)->L+3(B) (16%), H-6(B)->L+1(B) (15%)
42	271.04	0.0064	HOMO(B)->L+3(B) (75%)
43	267.54	0.0029	H-12(B)->LUMO(B) (53%)
44	263.82	0.0017	H-2(A)->L+3(A) (22%), HOMO(B)->L+5(B) (35%)
45	262.64	0.0104	HOMO(A)->L+7(A) (13%), H-13(B)->LUMO(B) (19%), H-12(B)->LUMO(B) (14%)
46	260.74	0.002	H-13(B)->LUMO(B) (25%), H-4(B)->L+2(B) (23%)

47	260.51	0.0039	HOMO(A)->L+7(A) (23%), H-12(B)->LUMO(B) (18%)
48	259.37	0.0132	HOMO(A)->L+7(A) (16%), H-13(B)->LUMO(B) (38%), H-4(B)->L+2(B) (19%)
49	257.23	0.0417	H-6(B)->L+1(B) (12%), H-4(B)->L+2(B) (17%)
50	251.36	0.0077	H-2(A)->L+1(A) (18%), H-14(B)->LUMO(B) (13%), H-5(B)->L+2(B) (12%)

---

### References:

- S1. M. Fischer and J. Georges, *Chem. Phys. Lett.*, 1996, **260**, 115.
- S2. S. Uchiyama, Y. Matsumura, A. P. de Silva and K. Iwai, *Anal. Chem.*, 2003, **75**, 5926.
- S3. J. R. Lakowicz, Principles of Fluorescence Spectroscopy, 3rd edn., *Springer Science*, 2006, 141-143.
- S4. X. Yu, J. Wan, S. Chen, M. Li, J. Gao, L. Yang, H. Wang, D. Chen, Z. Pan and J. Li, *Talanta*, 2017, **174**, 462–467.
- S5. Y. Ma, Y. Zhang, X. Liu, Q. Zhang, L. Kong, Y. Tian, G. Li, X. Zhang and J. Yang, *Dyes Pigm.*, 2019, **163**, 1–8.
- S6. P. Sakthivel, K. Sekar, S. Singaravel and G. Sivaraman, *ChemistrySelect*, 2019, **4**, 3817–3822.
- S7. A. Kathiravan, A. Gowri, T. Khamrang, M. D. Kumar, N. Dhenadhayalan, K.-C. Lin, M. Velusamy and M. Jaccob, *Anal. Chem.*, 2019, **91**, 13244–13250.
- S8. Y. Han, J. Zhao, H. Yang, X. Huang, X. Zhou, T. Hui and J. Yan, *J. Mol. Struct.*, 2020, **1217**, 128395.
- S9. S. Guo, G. Zhang, F. Chen, Y. Ni, J. Huang, L. Kong and J. Yang, *New J. Chem.*, 2021, **45**, 21327–21333.
- S10. S. A. Azad, A. Bera, J. Samanta, N. Sepay, R. Jana, C. K. Pal, M. R. Molla, D. Maiti and S. Samanta, *Chem. Eur. J.*, 2023, DOI:10.1002/chem.202303287.
- S11. N. Yan, J. Song, F. Wang, L. Kan, J. Song, W. Wang, W. Ma, W. Zhang and G. He, *Chin. Chem. Lett.*, 2019, **30**, 1984–1988.
- S12. H. Li, R. Jia and Y. Wang, *Spectrochim. Acta A Mol. Biomol. Spectrosc.*, 2020, **228**, 117793.